Optimised aluminium vehicle front section

Public version

ika Report 33390

Institut für Kraftfahrwesen Aachen
Body Department

Final report

Optimised aluminium vehicle front section

Project number
33390

Contractor:

European Aluminium Association
12, avenue de Broqueville
B- 1150 Brussels

Project manager:

Project engineer:

Dipl.-Ing. Georgi Chakmakov

Dipl.-Ing. Markus Franzen

Dipl.-Ing. Sven Faßbender

Univ.-Prof. Dr.-Ing. Henning Wallentowitz Dipl.-Ing. Peter Urban

Aachen, August 2006

Phone: +49 / (0)241 / 80-25 600 Fax: +49 / (0)241 / 80-22 147
e-mail: office@ika.rwth-aachen.de internet: http://www.ika.rwth-aachen.de
Office: ika, Steinbachstraße 7, D-52074 Aachen Mail address: ika, RWTH Aachen, D-52056 Aachen

Contents

1 Introduction

With continuously rising fuel costs and vehicle weights, the application of light weight materials for automotive engineering is a much discussed approach to improve vehicle economy. In this context, the car body offers effective mass saving potential. Up to now, light weight metals have hardly been used for load bearing structures of compact and middle class car bodies, although fuel consumption commonly is often a major selling point for these vehicle classes. In addition, the effect of weight reduction on fuel consumption is most significant in city traffic, where cars of smaller classes are frequently used.

Within this study the application of aluminium for the structural components of the front section of a C-class vehicle is analysed by the Institut für Kraftfahrwesen Aachen (ika) in cooperation with the European Aluminium Association (EAA). The aim is to develop and numerically analyse two concepts for an aluminium front section. The conservative aluminium concept is developed considering the exact design space limitations of a steel reference vehicle. For the progressive aluminium concept the design space is expanded, as far as possible with respect to the major package components of the reference vehicle, in order to achieve more design freedom and enable innovative ideas. Both aluminium concepts shall offer at least the same structural performance as the reference structure. Under this constraint a high level of weight reduction is intended.

This report summarises the development strategy, the findings and the results of the study. In a first step, the real reference structure is analysed and represented as a finite element model for later comparison with the virtually developed aluminium concepts. Subsequently, each aluminium concept is described in a separate chapter. The report closes with an evaluation of the aluminium concepts in comparison to the steel reference structure regarding structural performance.

2 Development strategy

The aim of this study is to assess and evaluate the performance and the weight saving potential of aluminium as a material for crash-relevant, structural parts of the front section of a C-class vehicle. This is done by developing and analysing aluminium concepts of these parts. The front structure of a state-of-the-art steel body is chosen as a reference. The static performance in bending and torsion as well as the crash performance in a frontal crash against a rigid barrier of this steel structure is set as the minimum requirement for the aluminium structure concepts that are joined to the rear part of the steel reference front section.

As shown in Fig. 2-1, two different concept development approaches, a conservative and a progressive one, are planned with the above-mentioned boundary conditions. For the conservative concept the package of the reference vehicle must not be changed. This results in minor design-freedom, since many package components are adapted to the steel body design. In order to extend the design freedom and enable more innovative design ideas, minor changes in package are allowed for the progressive concept. The changes only affect components that can be easily adapted to the body structure, such as pipes, hoses and tanks or components that can be moved to another position. Design space limitations, such as wheel-envelopes and space requirements for engine, suspension and cooling system are considered for the progressive concept in the same way as for the conservative concept.

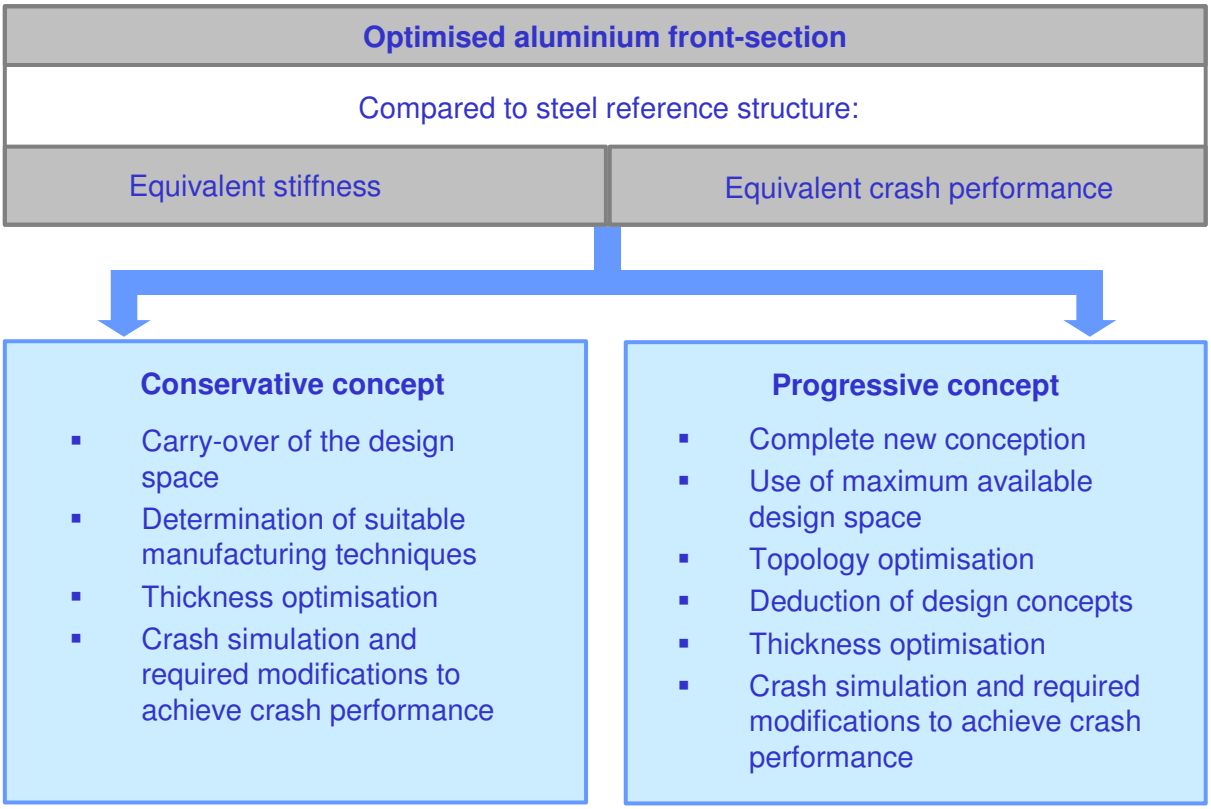

Fig. 2-1: Development strategy for progressive concept and conservative concept

For both approaches the concept development focuses on parts of major importance to the structural performance. These are parts that absorb most of the energy during a crash and contribute to the stiffness of the front section and the whole body respectively. In addition, these parts should allow for the application of different manufacturing and joining techniques. The above-mentioned requirements are fulfilled mainly by the following parts:

- Lower longitudinal beam
- Upper longitudinal beam
- Strut tower

3 Steel reference structure

Within this study solely the crash-relevant, structural parts of the front section are re-designed as aluminium parts. A steel reference structure is required for two reasons. Firstly, it forms the reference structure for the comparative assessment in structural performance and weight of the newly designed aluminium structures. Secondly, the rear part of the steel front section provides an interface to which the re-designed aluminium parts are joined.

3.1 Selection of reference vehicle

For the selection of the reference vehicle a benchmark is performed in the beginning of this study. The benchmarking and assessment process is shown in Fig. 3-1.

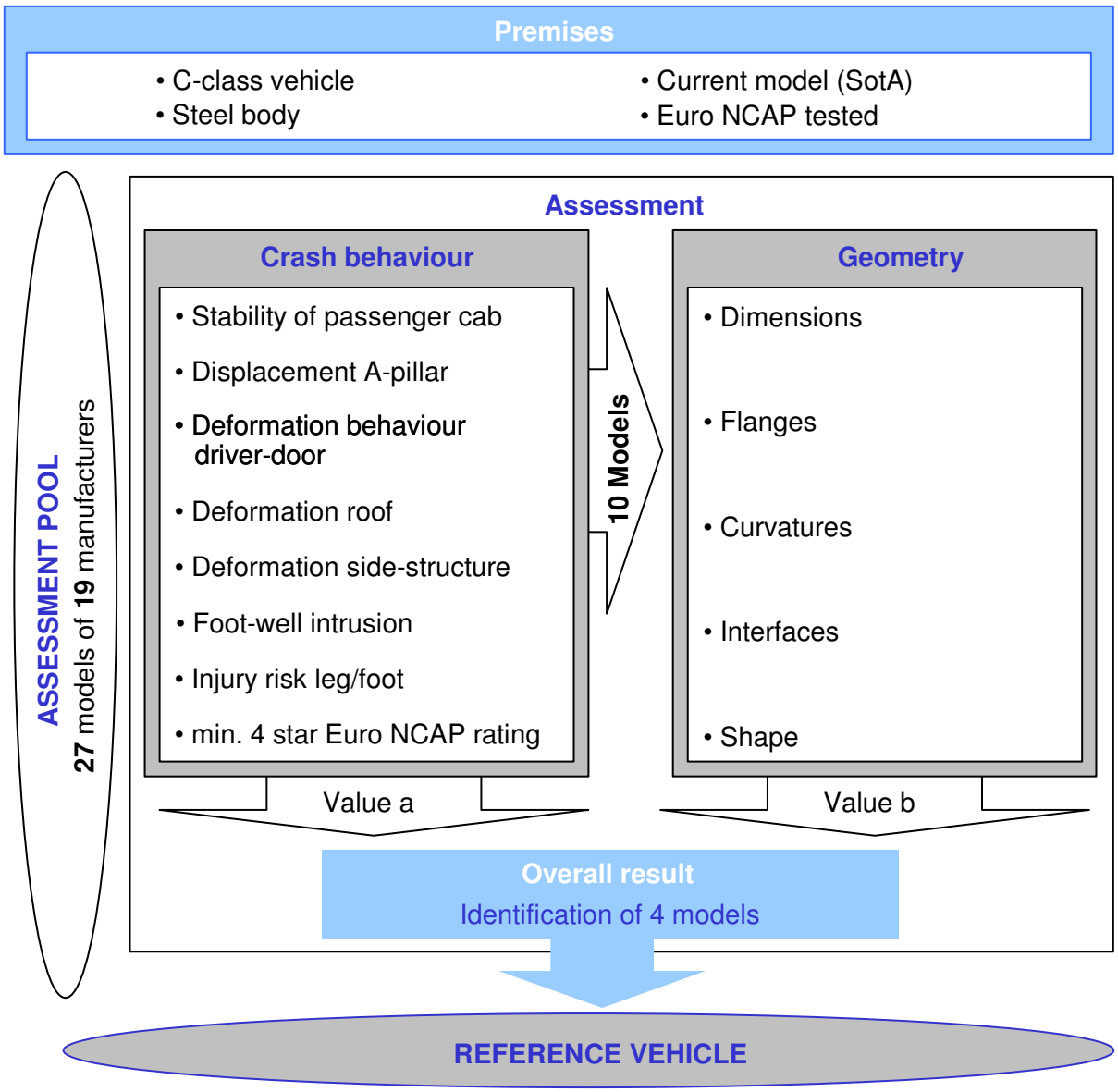

Fig. 3-1: Benchmarking and assessment of potential reference vehicles

Most of the premises for the potential reference vehicles directly result from the aims of this study. C-class vehicles are considered exclusively, since aluminium front sections are not established for this class. To enable a material substitution, the original vehicle has to have a steel body. The design of that steel body should be state-of-the-art, in order to represent up-to-date requirements. Therefore a current model is required. In addition, all models have to be Euro NCAP tested, since the testing results can provide input for the assessment of the structural performance.

27 models of 19 manufacturers fulfil the criteria of the basic premise. For the selection of the reference vehicle a closer assessment of these models is required. The assessment mainly focuses on the dynamic structural performance and the geometry.

It is not only the dynamic structural performance that is assessed by the Euro NCAP rating values, but the results are influenced also by parameters like the restraint systems of the particular model, seat belt warnings etc. In order to determine the performance of the structural body parts, the deformation behaviour is analysed and evaluated by the Euro NCAP high-speed videos. Ten models with the best performance are considered further.

The applicability of the ten remaining models for a hybrid body design is analysed including the feasibility consideration of the steel-aluminium-interface and of the main member design. Thereby the number of remaining models can be reduced to four. The final decision for the reference vehicle is made by the project team considering, among other things, the production volume of the vehicle and the cost of the body. A model with high cubic capacity diesel engine and air conditioning is finally chosen as a reference vehicle, in order to consider the maximum package constraints.

3.2 Analysis of reference structure

The objective for the development of the aluminium parts is to achieve at least the same performance as the steel reference structure. Therefore, the status-quo of the performance of the reference structure has to be determined within experimental and numerical analyses. The numerical analyses are required for an effective comparison with the virtually developed aluminium parts, while the experimental analyses are used for the validation of the numerical reference model. Experimental and numerical analyses are carried out for static load cases to determine the stiffness and for a crash load case to determine the force transfer and energy absorption.

Within the analyses the front section is regarded as a sub-system, separated from the other body components. For the experimental analyses an entire body-in-white of the reference vehicle was purchased. As it is shown in Fig. 3-2, the front section is cut off directly behind the a-pillar. Adapter plates are welded to the cutting areas to enable the support of the front section at the test bench and at the crash-sled.

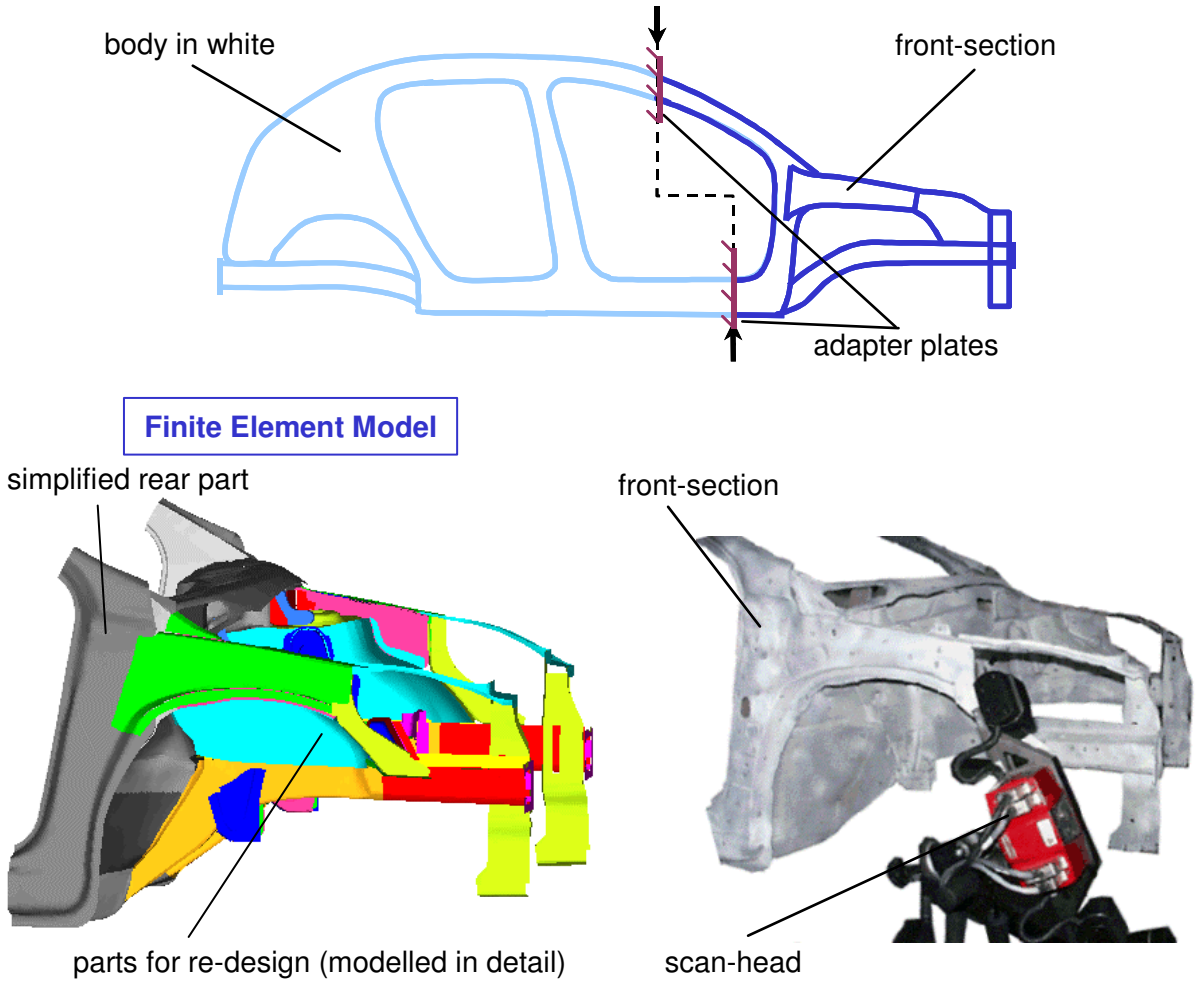

Fig. 3-2: Preparation of reference structure

To generate the finite element model, the reference front section is digitised with the three-dimensional-scanner-system ATOS II. The standard deviation of the recorded measuring point is less than 0.03 mm. Despite the use of the digitalisation, the translation into a well-meshed finite element model is rather complex. Therefore, the rear part and in some areas also the frontal part have been simplified. The major simplification is, that the rear part is built up symmetrically and that joining techniques are modelled for the frontal part only. The simplifications of the rear part are tolerable, since the rear part will be the same for the model of the reference structure and the re-designed aluminium concepts.

3.2.1 Static performance

For the experimental determination of the stiffness the reference structure is clamped to a horizontal span and supported at the adapter plates. The scheme of the test bench is shown in Fig. 3-3. Typically, for stiffness measurements of an entire car body the forces are applied to the strut towers. In the case of the front section the forces are applied to the crashbox supports at the end of the longitudinal beams. This is done in order to stress the whole front

section. In addition, the displacements at the strut tower would be very low, as the structure is clamped directly behind the strut tower resulting in a higher relative deviation.

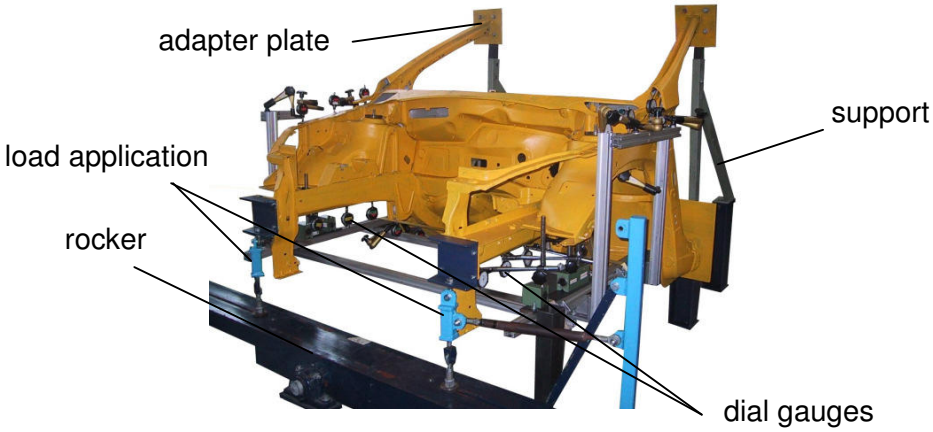

Fig. 3-3: Test bench set-up for experimental stiffness analysis

The applied forces per longitudinal beam amount to 917 N for bending and 2149 N for torsion. The torsional load is applied by a pair of forces via a rocker. The equivalent torque of the pair of forces is 2106 Nm. The vertical displacements are measured at different positions along the longitudinal beam by dial gauges. With the displacements the elastic curves of the longitudinal beam and, associated with the related forces, the bending and torsional stiffness can be determined. The elastic lines of the longitudinal beam are shown in Fig. 3-4 for bending and torsion for the left longitudinal beam.

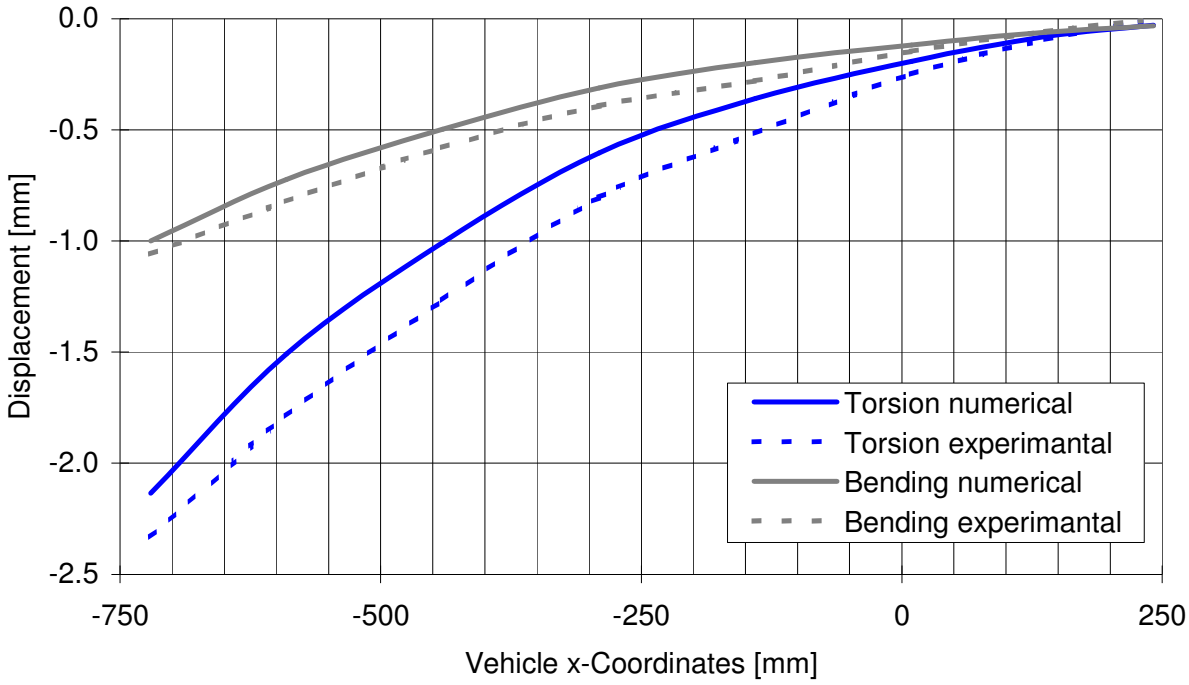

Fig. 3-4: Elastic deflection curves of longitudinal beam

The compliance of the test bench is subtracted from the measuring results. The elastic deflection line is used for the verification of the finite element model. As it can be observed in Fig. 3-4, the curvatures of the measured and calculated elastic lines compare well.

Since the detection of minor displacements is not critical in numerical calculations, the load cases bending and torsion with force application at the strut tower can be analysed based on the finite element model. The applied forces per strut tower amount to 5386 N for bending and 2567 N for torsion. The torsional load is applied by a pair of forces. The equivalent torque of the pair of forces is 3000 Nm. The results of all analysed load cases are shown in Fig. 3-5.

Load Case	Picture	Load	Analysis	Displacement	Stiffness
Bending (frontal)	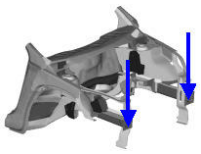	1834 N (2 x 917 N)	experimental	1.059 mm	1731 N/mm
			numerical	1.000 mm	1834 N/mm
Torsion (frontal)	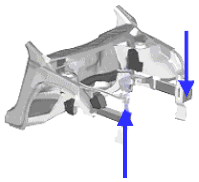	2106 Nm	experimental	2.332 mm	7723 Nm/°
			numerical	2.135 mm	8436 Nm/°
Bending (strut tower)	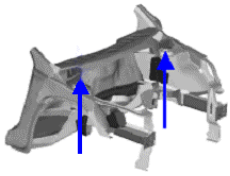	10772 N (2 x 5386 N)	experimental	---	---
			numerical	0.667 mm	16150 N/mm
Torsion (strut tower)	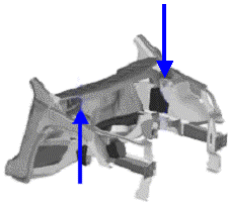	3000 Nm	experimental	---	---
			numerical	0.304 mm	100672 Nm/°

Fig. 3-5: Results of stiffness analyses for all load cases (reference front section)

Using the finite element model the stress distribution for the particular load cases can be calculated. The results are shown in Fig. 3-6, where the von-Mises-stresses are visualised by iso-surfaces of different colours, and the deformation is displayed with a scale factor of 50. For visualisation the maximum stress value is set to 30 N/mm^2. All areas of the front section where a von-Mises-stress of 30 N/mm^2 is exceeded are coloured in red. In addition, the maximum stresses are given for each load case.

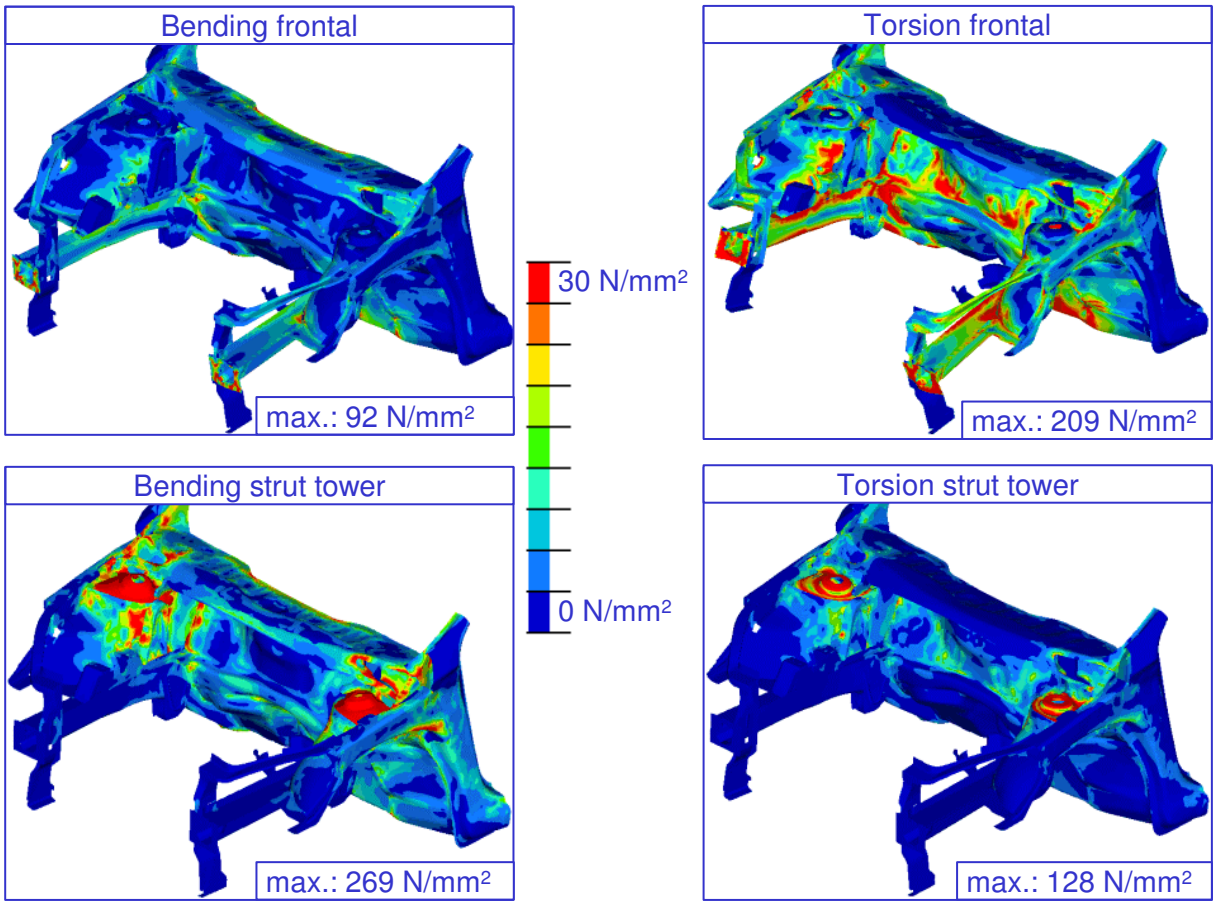

Fig. 3-6: Calculated stress distribution and maximum stresses (reference front section)

3.2.2 Crash performance

Like the static performance the crash performance is analysed in experiments and numerical simulations. The crash configurations of the experiments and the simulations are alike, too. As shown in Fig. 3-7, the reference front section is mounted to a crash sled by a support-construction using the adapter-plates at the end of the a-pillars.

The reference front section does not feature the frontal crossbeam and the engine. Realistic crash-behaviour of a body sub-system compared to the behaviour of the entire vehicle can only be reproduced, if the mass inertia of the engine and the frontal connection of the longitudinal beams are considered. Therefore the engine and the crossbeam are represented by substitute systems. The connection of the longitudinal beams is realised by a simple flat-bar, while the substitute engine system consists of a frame, which can be loaded with weights. The overall weight of the substitute engine system is 146.2 kg.

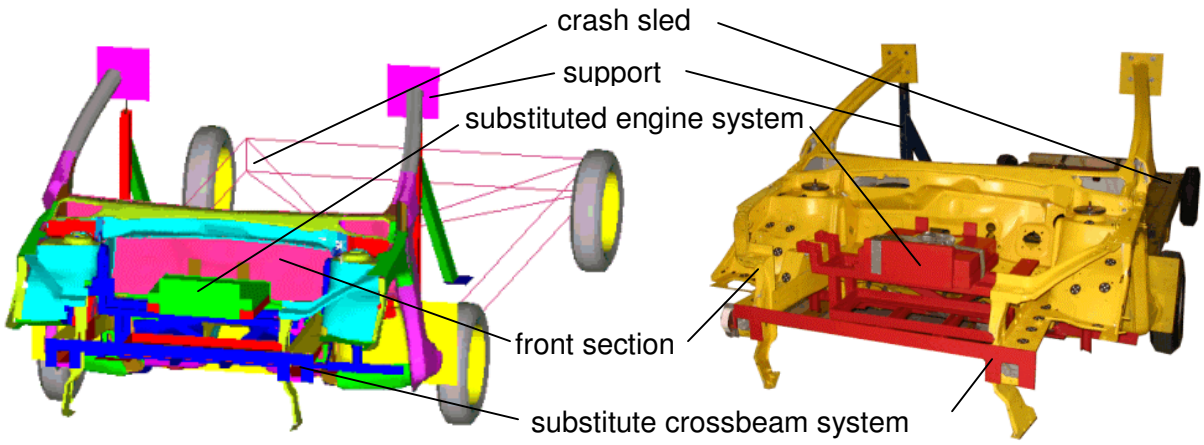

Fig. 3-7: Finite element model of the simulation and crash sled of the experiment

The analysed crash scenario for the front section is a straight impact against a planar, rigid barrier. The overall crash mass of the front section, the crash sled and the weights amounts to 1415 kg, which is equivalent to the total unloaded mass of the entire vehicle. The impact speed is 7.852 m/s or 28.27 km/h respectively. This results in a kinetic crash energy of 43.62 kJ.

For the quantitative evaluation of the experimental crash the crash sled or the rigid barrier respectively are equipped with acceleration, force and distance sensors. The force-deformation-curves and the dissipated energy derived from the sensor data and the simulation are shown in Fig. 3-8 and Fig. 3-9.

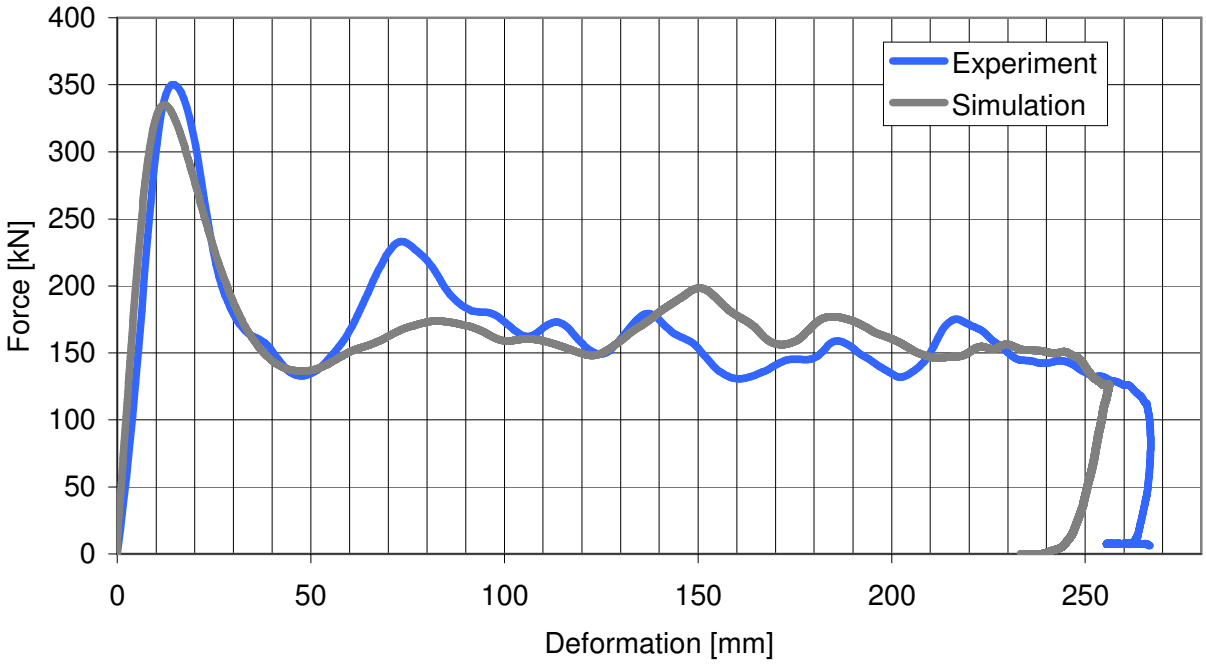

Fig. 3-8: Force versus deformation curve of experiment and simulation

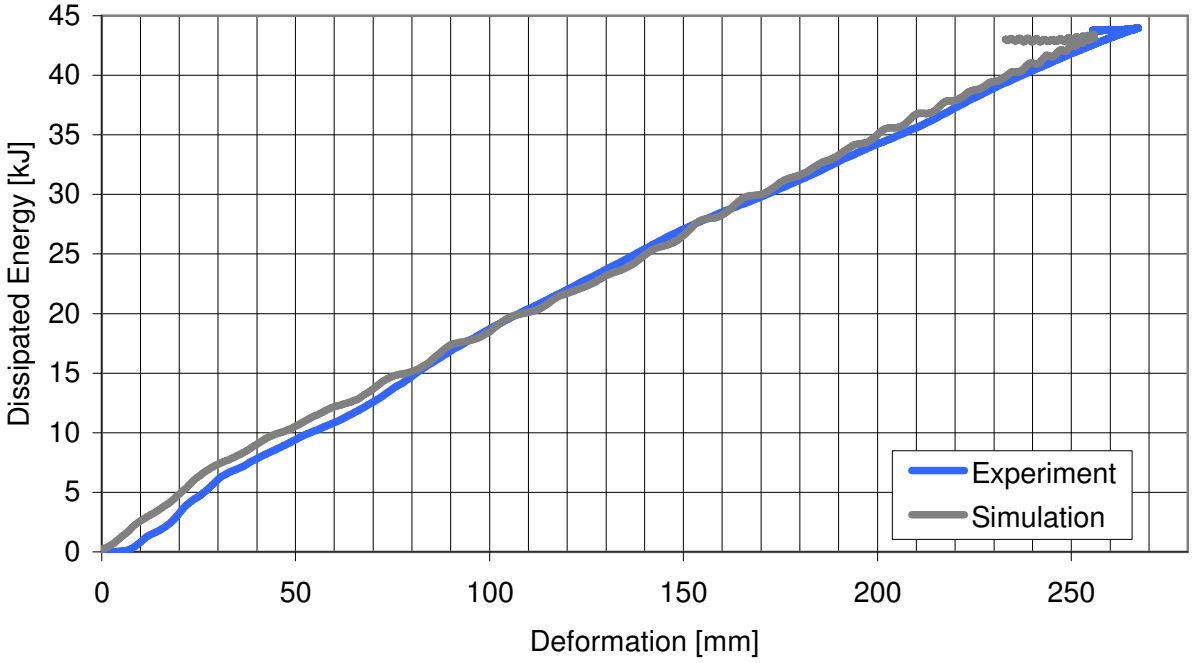

Fig. 3-9: Energy versus deformation plots of experiment and simulation

For the qualitative evaluation of the crash-behaviour two high-speed cameras record the experimental crash from the top and the left with a frame rate of 1000 per second. Equidistant states of these records are shown in Fig. 3-10 and Fig. 3-11 in comparison to simulation plots of the corresponding time.

The qualitative video data as well as the quantitative courses of deformation, force and energy are used for the validation of the finite element crash model. Regarding the deformation behaviour of the validated model in Fig. 3-10 and Fig. 3-11, a very good correlation between experiment and simulation can be observed. Even the unsymmetrical deformation behaviour of the left and the right longitudinal beam is shown by the finite element model of the reference front section.

While in the beginning of the deformation the left and the right longitudinal beam fail with to some extent regular buckling, a bending collapse of the left longitudinal beam is initiated at the tapering in the wheel house area after 30 ms. The right longitudinal beam shows regular buckling during the whole deformation. The unsymmetrical behaviour can be observed best in the top view of Fig. 3-11. Among others, one reason for the better crash-behaviour of the right longitudinal beam is the reinforcing effect of the engine support at the right wheel house area.

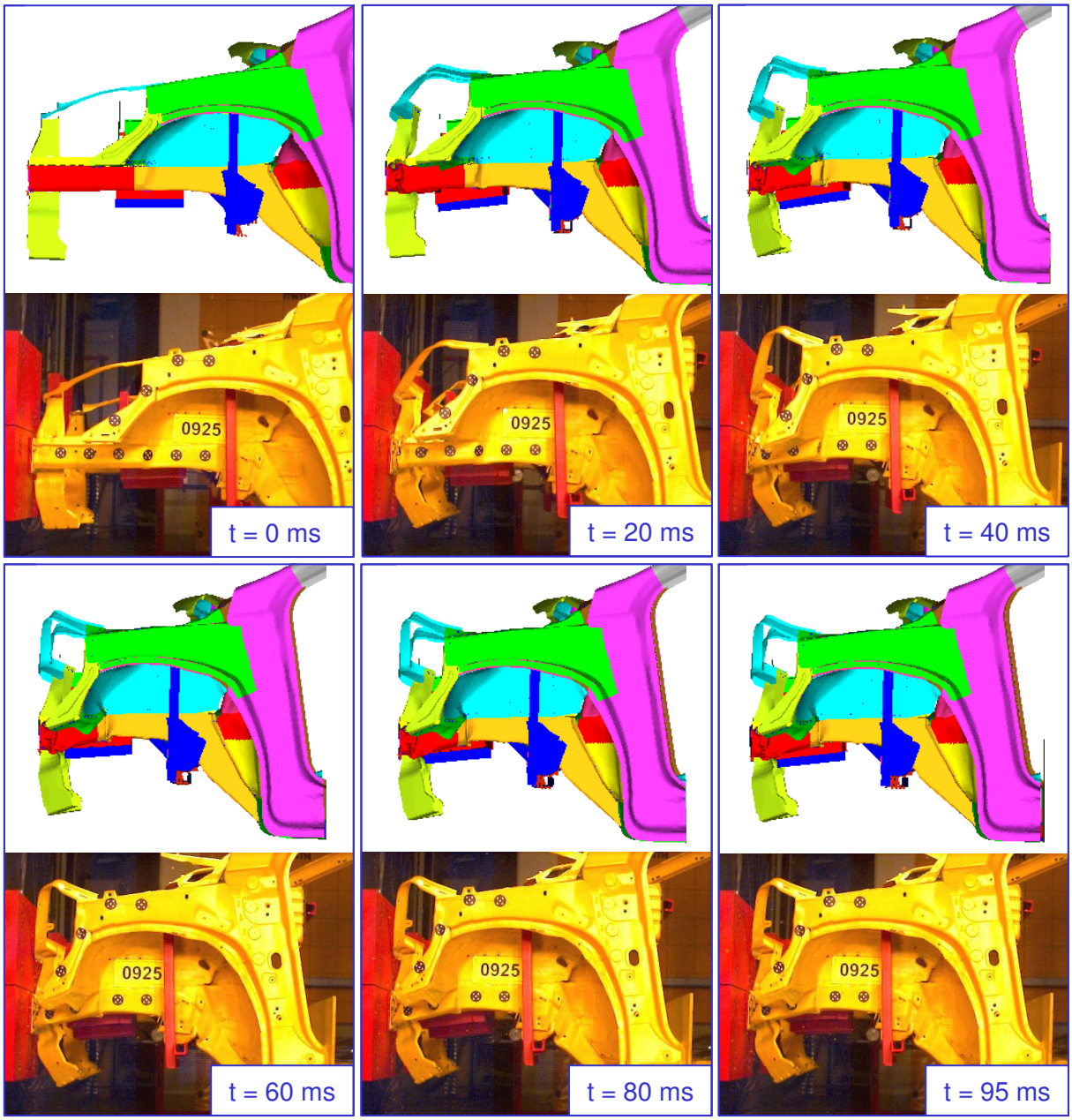

Fig. 3-10: Comparison of experimental and simulated deformation (left view)

In contrast to the deformation behaviour, minor differences between experiment and simulation can be observed in the quantitative data even after validation. Regarding the force-deformation-curves in Fig. 3-8, the first peak and valley of the experimental and simulated force still match well. The major difference between experiment and simulation is the height of the second peak and the total deformation. The second peak of the force-deformation-curve is about 50 kN higher in the experiment than in the simulation, while the simulated total deformation is about 10 mm shorter than the total deformation recorded in the experiment. The shorter simulated total deformation results in more demanding requirements for the development of the aluminium concepts, since the kinetic energy has to be dissipated over a shorter distance. This is because the simulation results of the aluminium concepts are

compared to the simulation results and not the experimental results of the steel reference structure.

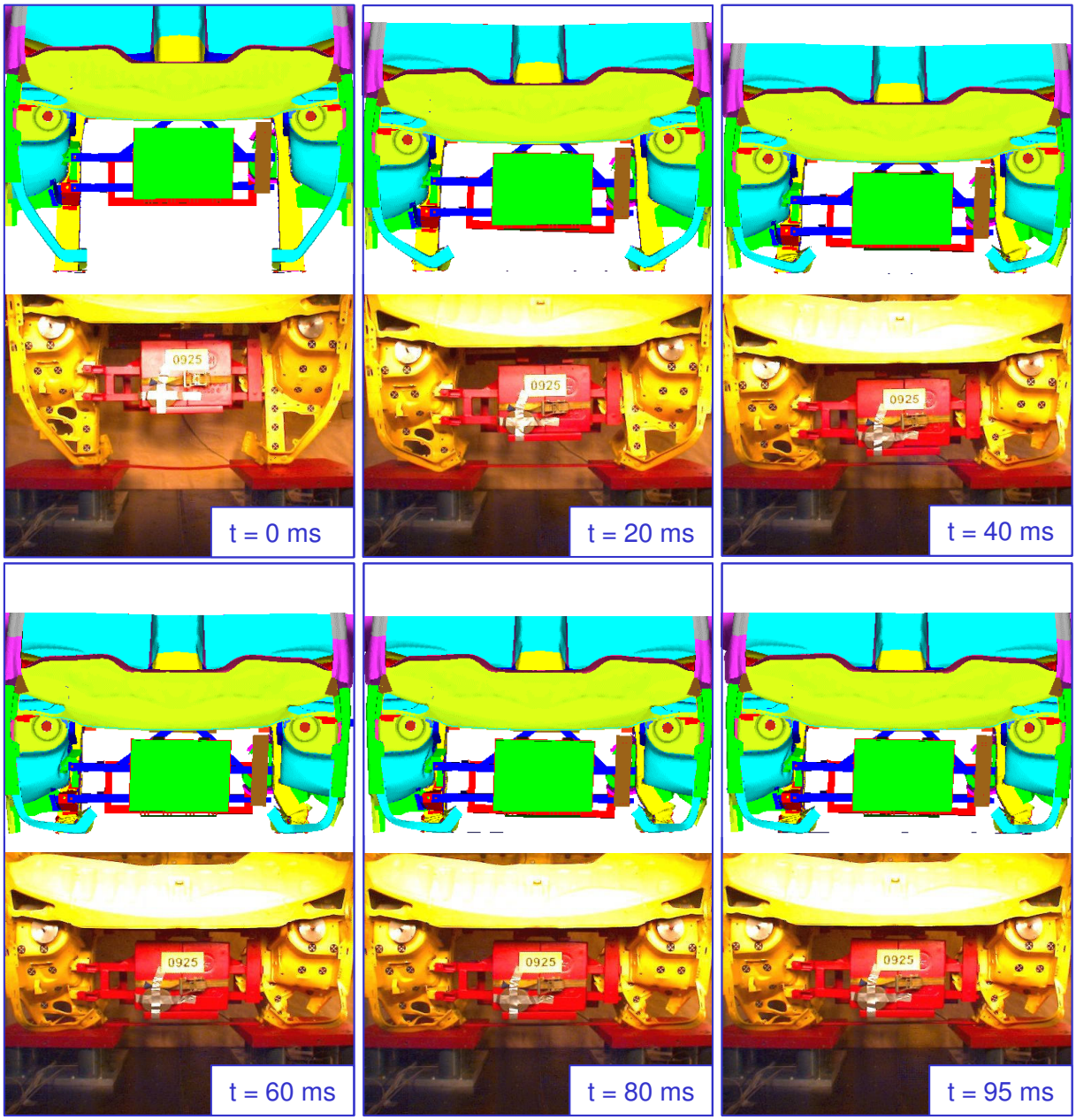

Fig. 3-11: Comparison of experimental and simulated deformation (top view)

Taking into consideration, that the finite element model of the reference structure is generated based on three-dimensional scans instead of CAD-data and the model is simplified, the achieved, quantitative results of the simulation after validation are more than satisfactory. This is also expressed by the good correlation of the dissipated energy versus deformation curves of simulation and experiment that are shown in Fig. 3-9.

4 Progressive concept

As described in chapter 2, within this study a progressive and a conservative approach for the development of an aluminium front section are investigated. The following sub-chapters describe the development and evaluation process of the progressive aluminium concept.

4.1 Design approach

The aim of the progressive design approach is to develop a design concept for an aluminium front section with an innovative shape. An important technique used to determine an appropriate arrangement of components is topology optimisation. Depending on given static load cases an optimised material distribution concerning stiffness and weight is calculated within a specified design space. The design space, modelled with solid elements, and the load cases considered for the development of the progressive aluminium concept are shown in Fig. 4-1.

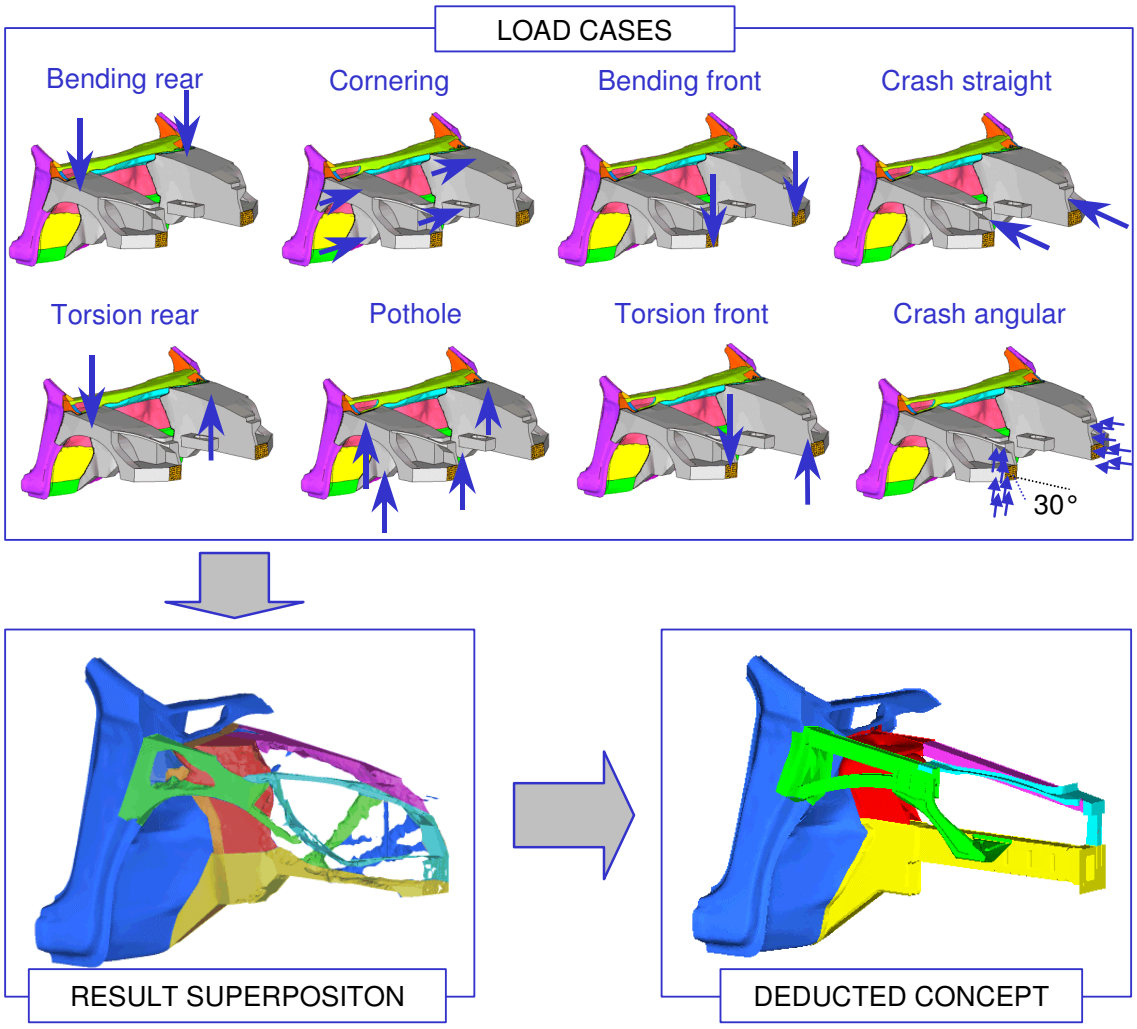

Fig. 4-1: Concept development by use of topology optimisation

Fig. 4-1 also shows the result of the topology optimisation for the right side of the front section, where significantly identified components are marked by colouring. Based on these results, first concepts for the aluminium front section can be deducted as shell models. Detailed definition of the progressive concept is done in an iterative process of multi-disciplinary optimisation and a review of the fulfilment of the crash requirements. Due to the crash requirements a wheel arc cannot be left out, although the topology optimisation does not show the need for material in that area.

4.2 Concept Specification

The final version of the progressive aluminium front section concept is shown in Fig. 4-2. With respect to the shape of the particular part, an applicable manufacturing technique is chosen. Aluminium offers a variety of different manufacturing techniques for body engineering, such as deep-drawing, extrusion or casting. Especially castings and extrusions allowing easy integration of parts, which can be beneficial in terms of cost, strength and performance aspects. The different manufacturing techniques require adequate alloys. Alloys used for the aluminium concepts of this study are Ac-300™ (AA 6014) for deep-drawing parts, AA 6060 for extrusions and A356 (AlSi7Mg) and C 448™ (AlSi10Mg) for castings.

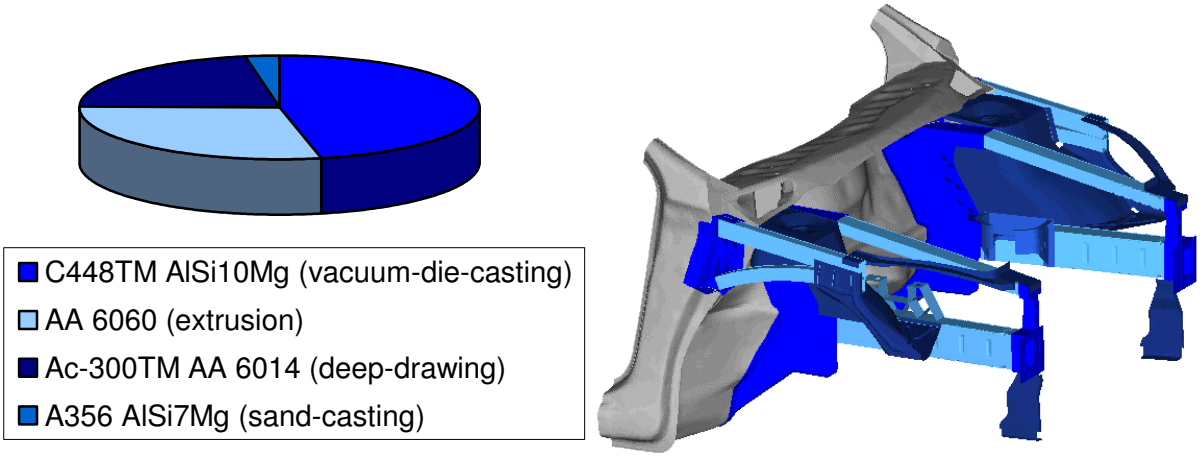

Fig. 4-2: Progressive aluminium concept with alloys used

For detailed information on the single parts of the progressive concept please see appendix. The total number of parts is reduced from 43 of the steel reference front section to 30 of the progressive aluminium concept. Examples for high part integration are the extruded engine support and the gear box support casting. These parts are shown in Fig. 4-3 compared to the corresponding steel designs.

The use of different manufacturing techniques and the hybrid steel-aluminium design of the progressive front section concept require a variety of joining techniques. In order to prevent contact-corrosion, insulating adhesive is applied at each contact zone between aluminium and steel. This adhesive does not contribute to the structural performance of the joint, but it

provides a galvanic insulation of the different materials and prevents any electrolyte, such as water, from entering into the joint seams. The structural connection between aluminium and steel is realised by self-piercing rivets. Self-piercing rivets are also used for connections between aluminium parts that are accessible from both sides. For single side accessible connections between aluminium parts MIG-welding is used.

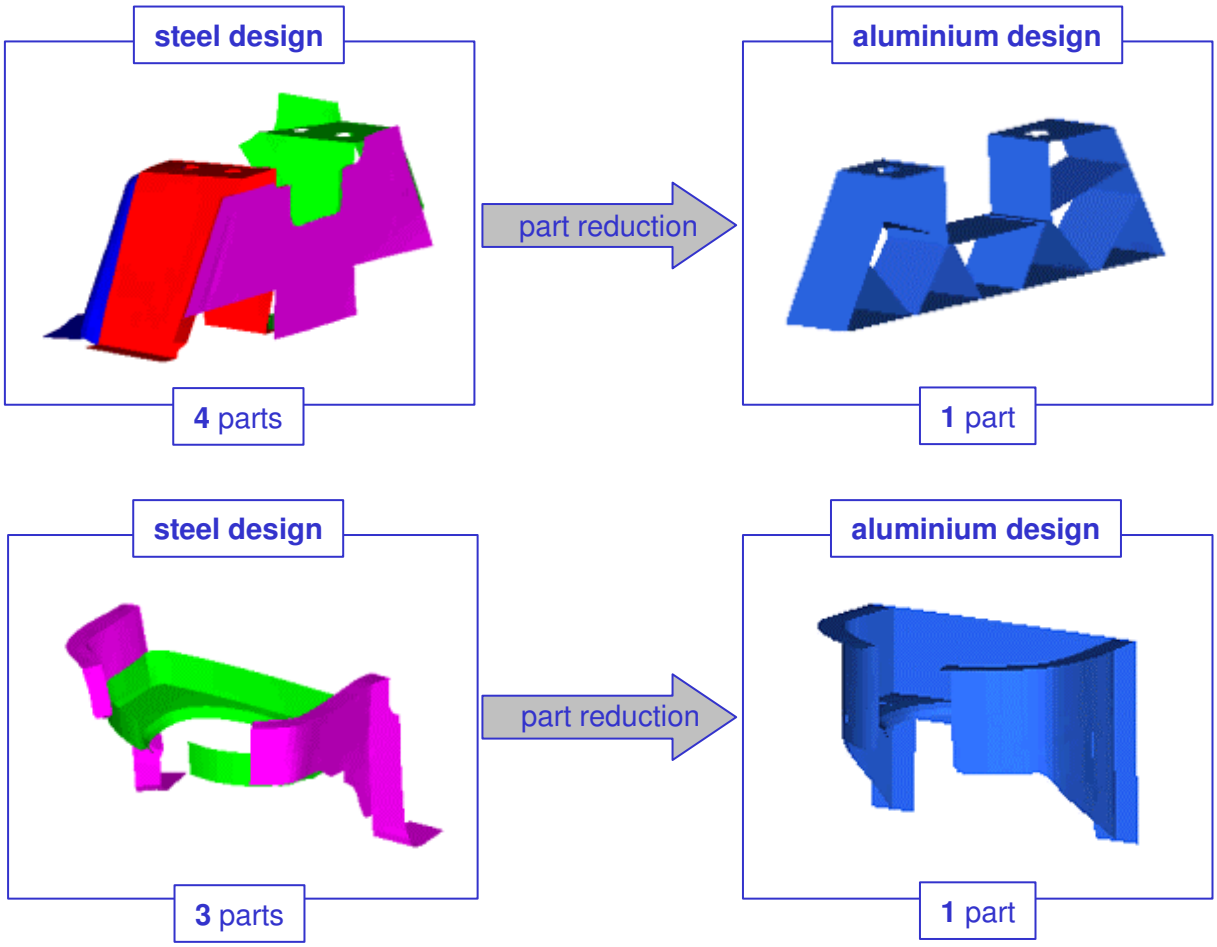

Fig. 4-3: Part-integration using extrusions and castings

4.3 Performance

The weight of the re-designed front section parts is reduced form 36.27 kg in the steel reference front section to 21.54 kg in the progressive aluminium front section. This is a weight saving of 14.73 kg or 40.61 %. For all load cases analysed the progressive aluminium concept achieves at least the performance of the steel reference structure. In most of the load cases the performance of the steel reference structure is even exceeded.

4.3.1 Static performance

In Fig. 4-4 the levels of stiffness for the different static load cases of the progressive aluminium concept are shown. The levels of stiffness are determined using the calculated displace-

ments at the application points numerically and the corresponding forces or torques respectively.

Load Case	Picture	Load	Analysis	Displacement	Stiffness
Bending (frontal)	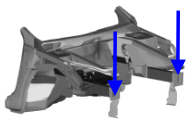	1834 N (2 x 917 N)	numerical	1.000 mm	1834 N/mm
Torsion (frontal)	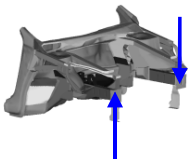	2106 Nm	numerical	1.926 mm	9351 Nm/°
Bending (strut tower)	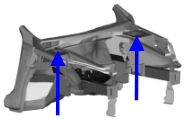	10778 N (2 x 5386 N)	numerical	0.579 mm	18604 N/mm
Torsion (strut tower)	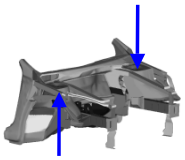	3000 Nm	numerical	0.249 mm	122909 Nm/°

Fig. 4-4: Results of stiffness analysis for all load cases (progressive concept)

Except for the load-case “Bending (frontal)”, which shows the same stiffness, all levels of stiffness are increased in comparison to the steel reference front section. The increase in stiffness is between 11% and 22% depending on the load case. The most important load cases for an entire vehicle are bending and torsion at the strut tower. If, in contrast to the requirements of this study, minor performance decrease in the load case “Bending (frontal)” was tolerable, the increase in stiffness of the other load cases could be used for the reduction of sheet thickness and finally result in further weight reduction.

By means of numerical simulation the stress distribution for the particular load cases can be calculated, as well. In Fig. 4-5 the von-Mises-stresses of the different load cases of the progressive concept are visualised by iso-surfaces of different colours, and the deformation is displayed with a scale factor of 50. The maximum stress value is set to 30 N/mm^2. All areas of the front section where a von-Mises-stress of 30 N/mm^2 is exceeded are coloured in red. In addition, the maximum stresses are given for each load case.

In comparison to Fig. 3-6, where the stress distribution in the steel reference structure is shown for the same load cases, it can be qualitatively observed, that the stresses in the progressive aluminium concept are lower. In addition, compared to the steel reference front section, the maximum stresses in the progressive concept are reduced by 33% to 51%, depending on the particular load case. The high peak stresses of the load cases “Torsion frontal” and “Bending strut tower” are not critical in terms of strength limit of the aluminium alloys used, since they occur in the steel part of the front section.

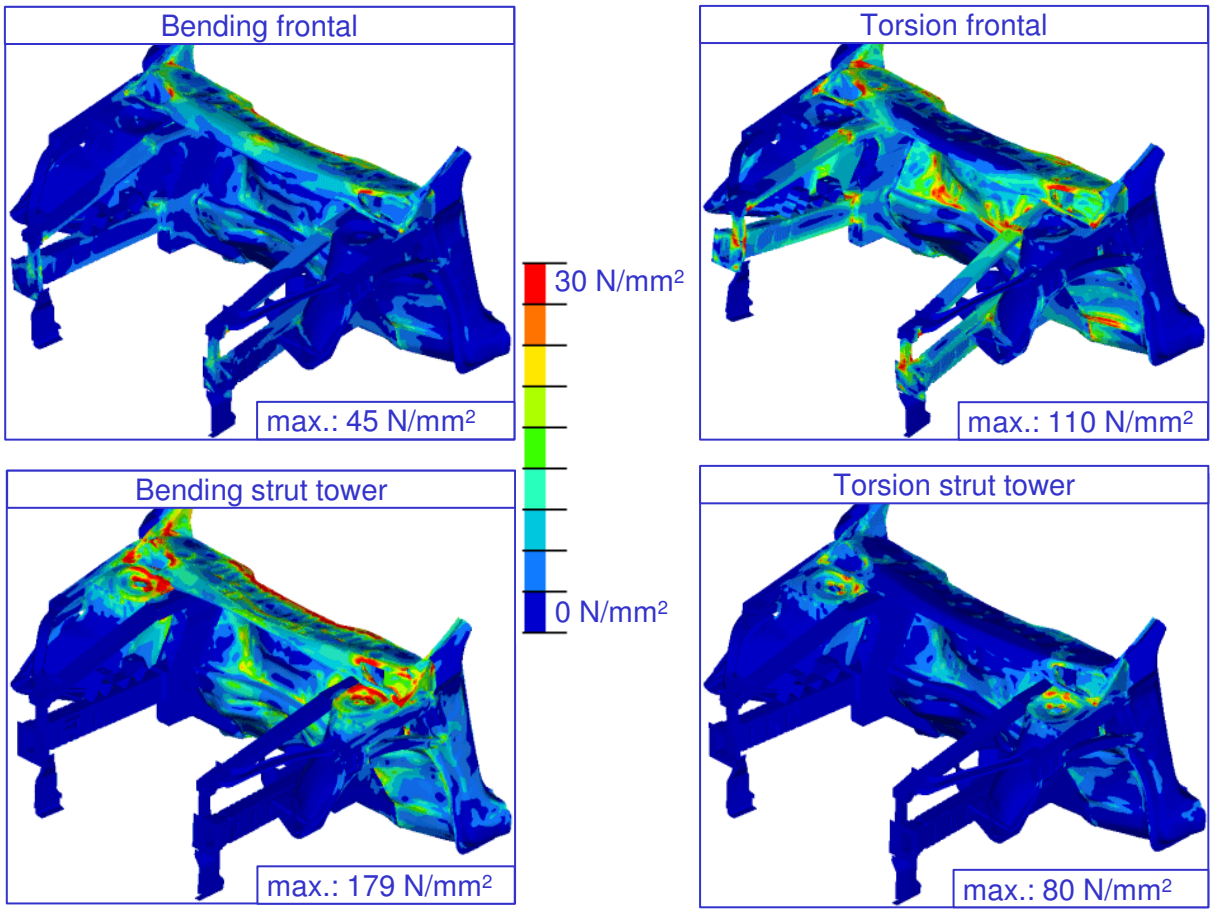

Fig. 4-5: Calculated stress distribution and maximum stresses (progressive concept)

4.3.2 Crash performance

To compare the steel reference structure to the progressive aluminium concept on an equal basis, the crash configuration and all additional settings of the solver are the same as for the crash simulation of the reference structure, described in chapter 3.2.2. Of course, the total crash mass is 1400 kg instead of 1415 kg, since the weight of the aluminium front section is reduced by 14.73 kg. As a result, the kinetic energy that has to be absorbed amounts to 43.16 kJ.

In contrast to the static performance, the crash performance of the different front sections cannot directly be evaluated by a single value such as stiffness or maximum stresses. All front sections have to withstand a straight impact (0% offset) against a planar, rigid barrier with a speed of 7.852 m/s or 28.27 km/h respectively. Consequently, the energy that has to be absorbed is default and therefore fails as a direct criterion. It can only be evaluated, in which way the energy is absorbed. This can be done by analysing the force-deformation-curve and the dissipated energy, shown in Fig. 4-6 and Fig. 4-7, as well as the deformation behaviour of the structure. For the visualisation of the deformation equidistant plots of the deforming progressive aluminium concept are shown in Fig. 4-8.

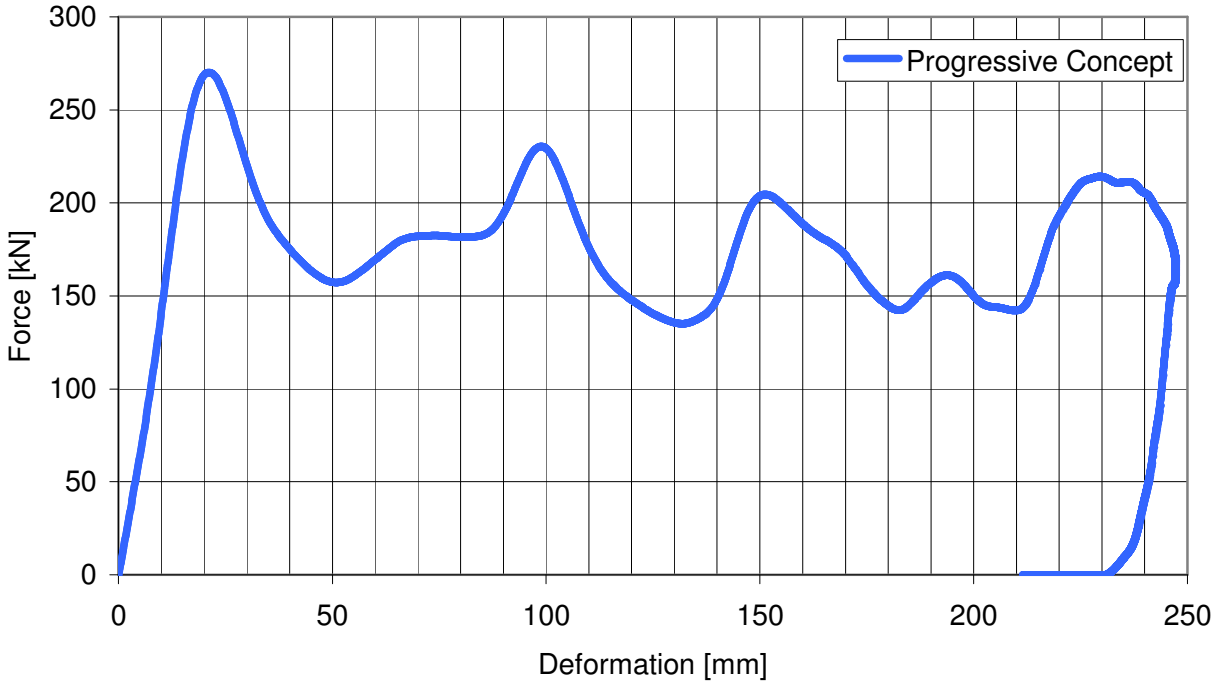

Fig. 4-6: Force versus deformation curve of progressive concept

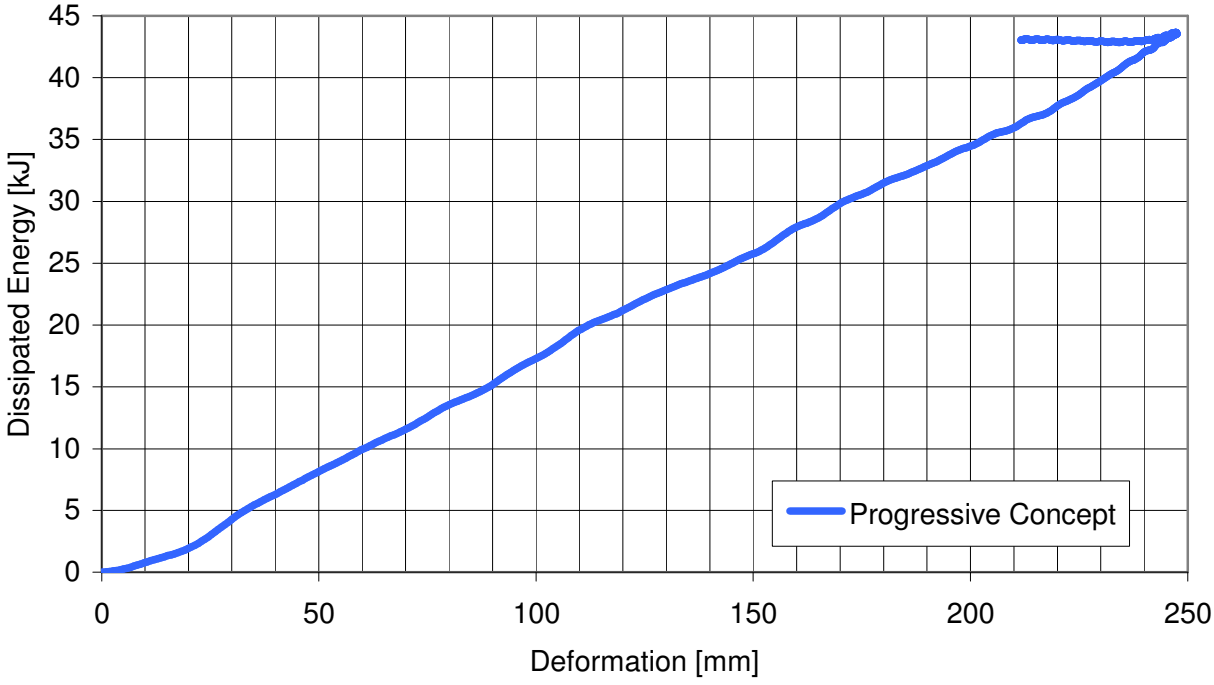

Fig. 4-7: Energy versus deformation plot of progressive concept

Regarding the force-deformation-curve in Fig. 4-6 it can be observed, that the difference between the average and the maximum deformation force is relatively small. The deformation

force does not decrease substantially after the first peak, which represents the buckling load. This is an indication for a high level of efficiency in energy absorption, since the optimum level of energy absorption is achieved by a rectangular force-deformation-curve, where the average deformation force is equal to the buckling load.

The higher level of efficiency in energy absorption has an effect on the total deformation. The total deformation from the frontal crash of the progressive concept is 247 mm, which is 9 mm less than the total deformation of the steel reference structure. This means, that less deformation is required to absorb the kinetic energy. As a result, the progressive aluminium concept has a reserve in deformation space that can be used to absorb additional energy.

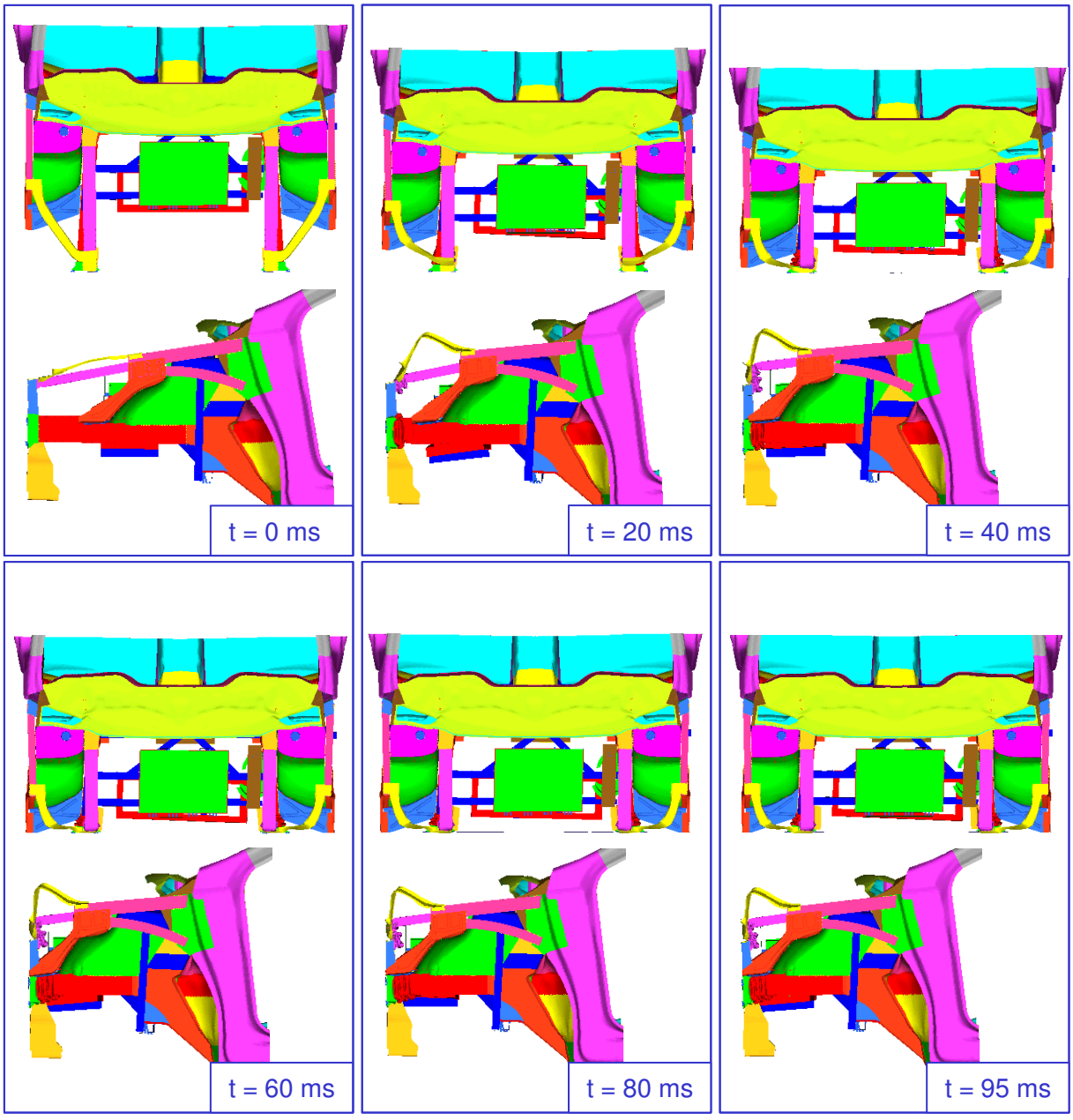

Fig. 4-8: Deformation of progressive concept (top and left view)

The discrete, clearly separated peaks and valleys of the force-deformation-curve indicate regular buckling of the upper and lower longitudinal beam. The regular buckling of profiles can also be observed in Fig. 4-8, which shows equidistant states of the deformation plots of the simulation. For each state the progressive aluminium concept is shown in the top and in the left view. The structural integrity of the front section is maintained throughout the entire crash. The deformation behaviour is rather symmetrical, and the longitudinal beams, that are the main energy absorbing parts, do not show an indication of collapse.

5 Conservative concept

As described in chapter 2, within this study a progressive and a conservative approach for the development of an aluminium front section are investigated. The following sub-chapters describe the development and evaluation process of the conservative aluminium concept.

5.1 Design approach

Since deviation from the package restrictions of the reference vehicle is not allowed within the conservative concept approach, the architecture of the aluminium front section is predefined to a large extent. Most of the redesigned aluminium parts have to be located in the same position and be shaped in a similar way as the corresponding steel parts.

For the design of the parts of the conservative concept technical expertise gained from the design of the progressive concept is used. As a result, the outer longitudinal beam (frame structure) is used as a carry-over part. The progressive concept shows that the combination of static and crash requirements can be fulfilled by using a hollow extrusion, which makes additional design space available by abandoning the flanges of the steel design. Therefore the front part of the main (lower) longitudinal beam of the conservative concept is designed in the same way. The rear part of the main longitudinal beam is realised by two deep-drawing parts that, due to manufacturability, have a different parting plane than the corresponding steel parts.

In order to reach a high level of part integration, the strut tower shall be designed as a cast part. Topology optimisation is used to determine the rough shape of the casting. Therefore the available design space in the area of the strut tower is modelled with solid elements and joined to the remaining parts of the front section. Since the topology optimisation for the conservative concept only relates to a limited area of the front section, being the strut tower, the number of considered load cases is reduced in comparison to the topology optimisation of the progressive concept. The design space for the strut tower within the front section for the conservative concept and the considered load cases are shown in Fig. 5-1.

In addition to the load cases “bending front”, “bending rear”, “torsion front” and “torsion rear”, that are known from the optimisation of the progressive concept, the load case “lateral compression” is included. It is known from the development of the progressive concept that lateral stiffness is important for the crash performance. This requirement is already considered in an early design phase by defining the static load case “lateral compression” for the topology optimisation as a substitute crash load case.

In order to illustrate the development process of the strut tower casting, Fig. 5-2 shows four design stages of the casting. Starting from a massive part filling the entire available design space an optimised material distribution with respect to the stiffness in the five considered load cases is calculated. Areas of major importance for the stiffness are visualised, and a coarse shape of the casting is deducted.

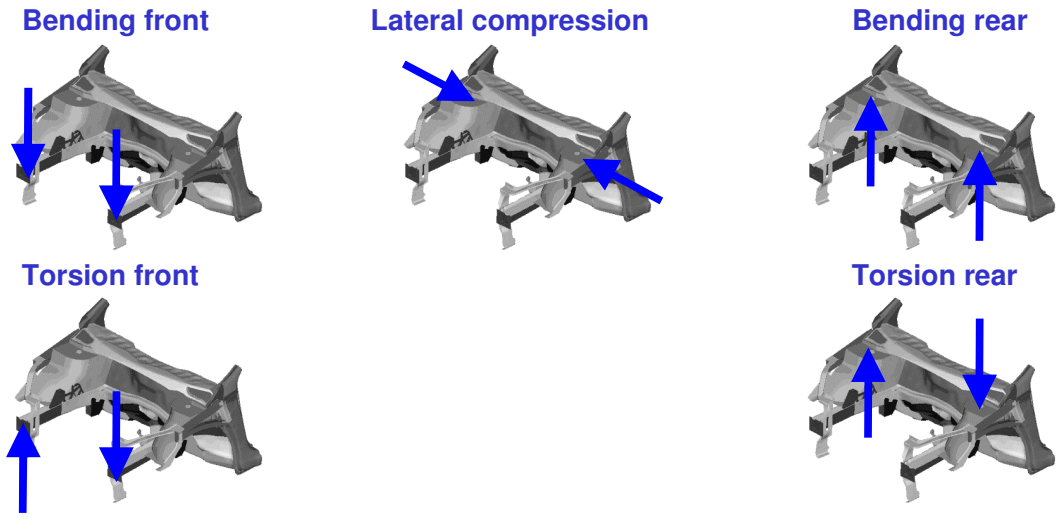

Fig. 5-1: Load cases for topology optimisation of strut tower casting

The coarse design deducted from the topology optimisation consists of a cast and a deep-drawn section for the connection to the firewall. The weight of the casting is further reduced by adding rips and at the same time reducing wall thickness. The location, shape and thickness of the rips are optimised iteratively.

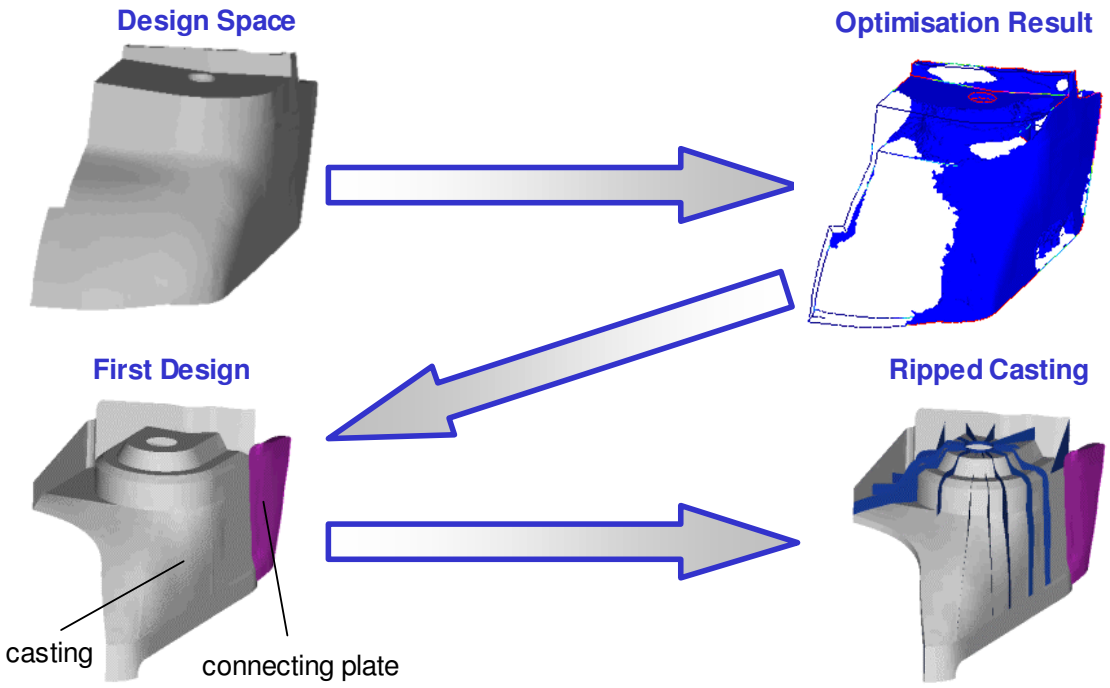

Fig. 5-2: Design stages of strut tower casting

Like the detailed conception of the progressive concept, also the detailed definition of the entire conservative concept is done in an iterative process of multi-disciplinary optimisation and review of the fulfilment of the crash requirements.

5.2 Concept Specification

The final version of the conservative aluminium front section concept is shown in Fig. 5-3, where the used aluminium alloys are coloured in different shades of blue. Each used alloy refers to an individual manufacturing technique. As with the progressive concept, Ac-300™ (AA 6014) is used for deep-drawing parts, AA 6060 for extrusions and A356 (AlSi7Mg) and C448™ (AlSi10Mg) for castings. As one can see, when comparing the steel reference front section to the conservative aluminium concept, it is possible to create a different design within the exact design space limitations of an existing reference body structure by choosing different applicable manufacturing techniques. Using the beneficial characteristics of each manufacturing technique with respect to the local requirements of the design offers room for improvement to the designer.

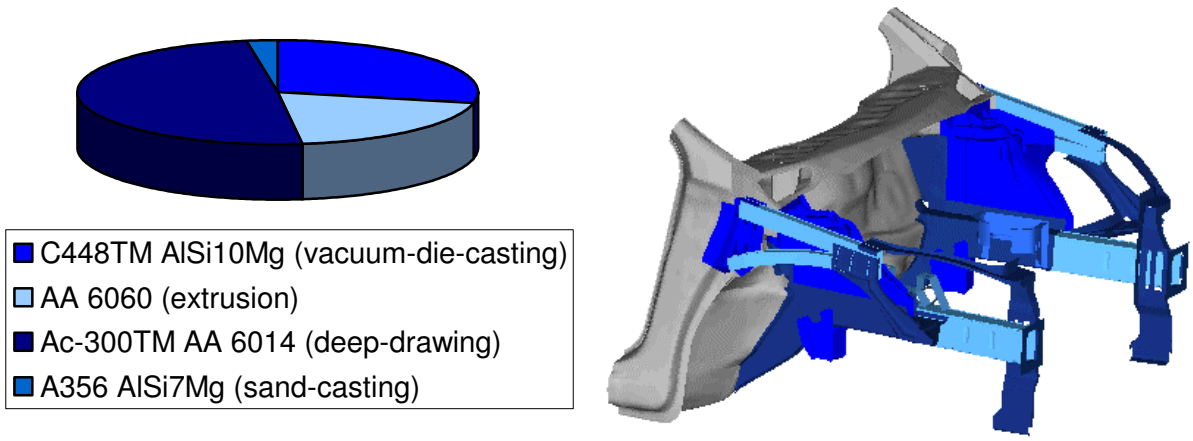

Fig. 5-3: Conservative aluminium concept with used alloys

Like the progressive concept, the conservative concept features a high level of part integration. In comparison to the steel reference structure the total number of parts is reduced from 43 to 30. For detailed information on the single parts of the conservative concept please refer to the appendix.

For inter-aluminium connections the used joining techniques are self-piercing rivets at locations that are accessible from both sides and MIG welding for partially accessible connections. Self-piercing rivets in combination with insulating adhesive are applied at the hybrid-material joints between aluminium and steel.

5.3 Performance

The weight of the re-designed front section parts is reduced from 36.27 kg of the steel reference front section to 23.60 kg of the conservative aluminium front section. This is a weight saving of 12.67 kg or 34.93%. For all analysed load cases the conservative aluminium concept achieves at least the performance of the steel reference structure. In most of the load cases the performance of the steel reference structure is even exceeded.

5.3.1 Static performance

In Fig. 5-4, the levels of stiffness for the different static load cases of the conservative aluminium concept are shown. The levels of stiffness are determined using the calculated displacements at the force application points and the corresponding forces or torques respectively.

Load Case	Picture	Load	Analysis	Displacement	Stiffness
Bending (frontal)	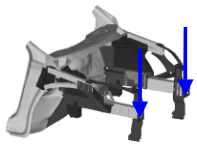	1834 N (2 x 917 N)	numerical	1.000 mm	1834 N/mm
Torsion (frontal)	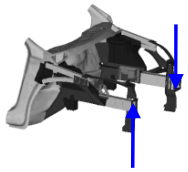	2106 Nm	numerical	1.985 mm	9028 Nm/°
Bending (strut tower)	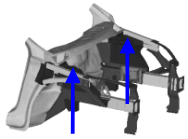	10778 N (2 x 5386 N)	numerical	0.599 mm	17983 N/mm
Torsion (strut tower)	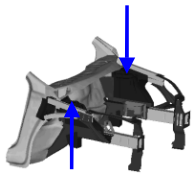	3000 Nm	numerical	0.261 mm	117258 Nm/°

Fig. 5-4: Results of stiffness analysis for all load cases (conservative concept)

Except for the load case “Bending (frontal)”, which shows the same stiffness, all levels of stiffness are a little bit lower than in the progressive concept, but increased in comparison to the steel reference front section. The increase in stiffness is between 7% and 16% depending on the load case.

Like for the progressive concept the load case “Bending (frontal)” is the critical load case. “Critical load case” in this regard means that all the effort put in the static dimensioning of the front section is necessary to achieve the required stiffness of the load case “Bending frontal”. As a result, the wall thickness of some parts have to be increased. If, in contrast to the

requirements set for this study, minor performance decrease in the load case “Bending (frontal)” was tolerable, since that load case is of minor importance to the stiffness of the entire body, the stiffness reserve of the other load cases could be used for the reduction of sheet thickness and as a result further weight reduction.

By means of numerical simulation the stress distribution for the particular load cases can be calculated. In Fig. 5-5, the von-Mises-stresses of the different load cases of the conservative concept are visualised by iso-surfaces of different colours, and the deformation is displayed with a scale factor of 50. The maximum stress value is set to 30 N/mm^2. All areas of the front section where a von-Mises-stress of 30 N/mm^2 is exceeded are coloured in red. In addition, the maximum stresses are given for each load case.

In comparison to Fig. 3-6 where the stress distribution in the steel reference structure is shown for the same load cases it can be qualitatively observed that the stresses in the conservative aluminium concept are lower.

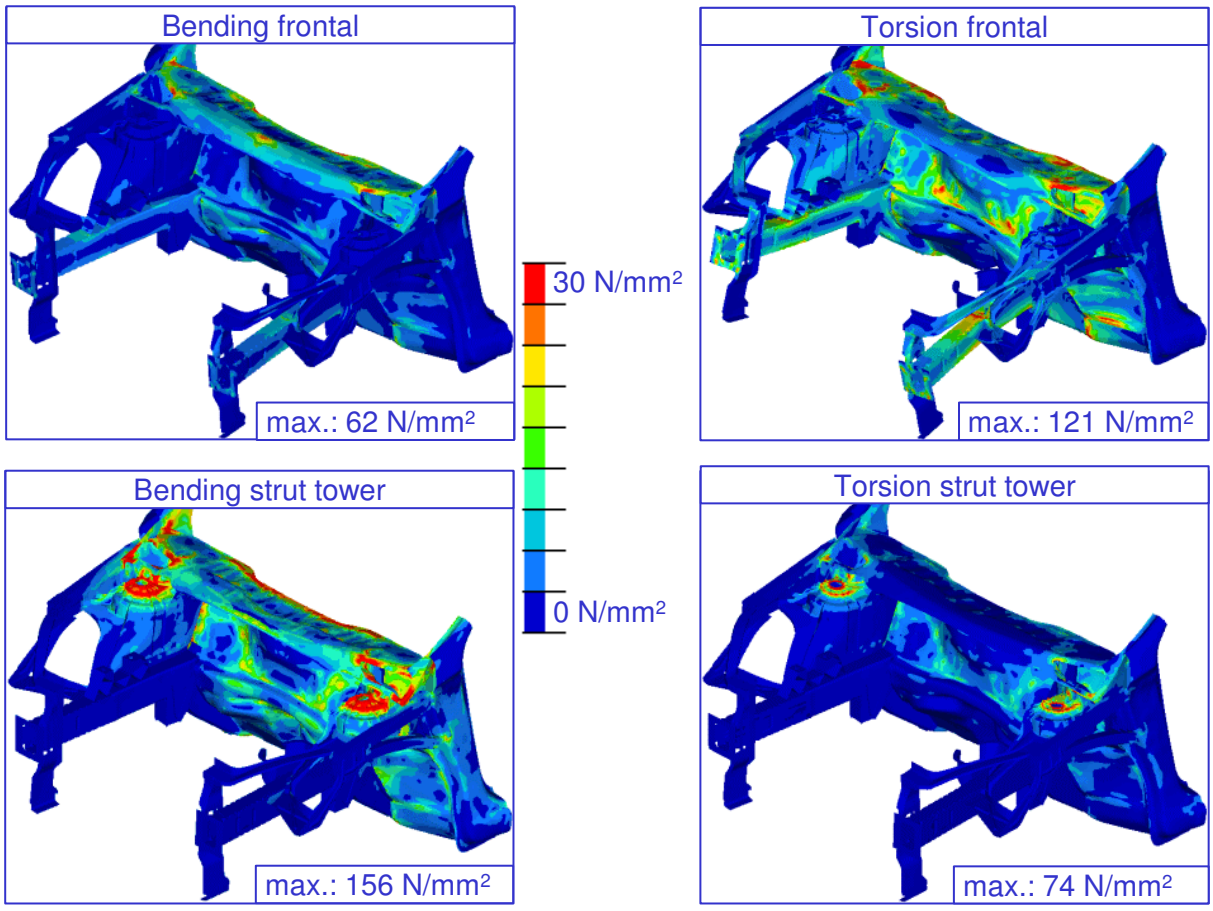

Fig. 5-5: Calculated stress distribution and maximum stresses (conservative concept)

In addition, compared to the steel reference front section, the maximum stresses in the conservative concept are reduced by 33% to 42%, depending on the particular load case. Regarding the load case “Bending strut tower” the high peak stress directly occurs at the

connection to the rigid spider of the force transmission point. Consequently, the value calculated is excessive and expected to be lower in reality.

5.3.2 Crash performance

The crash configuration for the numerical crash simulation of the conservative aluminium concept and all settings of the solver are the same as for the simulation of the steel reference vehicle and the progressive aluminium concept.

The conservative aluminium concept is subjected to a planar frontal impact against a rigid barrier with an impact speed of 7.852 m/s or 28.27 km/h respectively. Of course, the total crash mass is 1403 kg instead of 1415 kg or 1400 kg respectively, since the weight of the conservative aluminium front section is reduced by 12.67 kg in comparison to the steel reference structure. As a result, the kinetic energy that has to be absorbed amounts to 43.25 kJ.

For quantitative assessment of the crash performance of the conservative aluminium concept the force-deformation-curve and the dissipated energy that are shown in Fig. 5-6 and Fig. 5-7 are used. For the visualisation of the deformation and to enable qualitative assessment, equidistant plots of the deforming conservative aluminium concept are shown in Fig. 5-8.

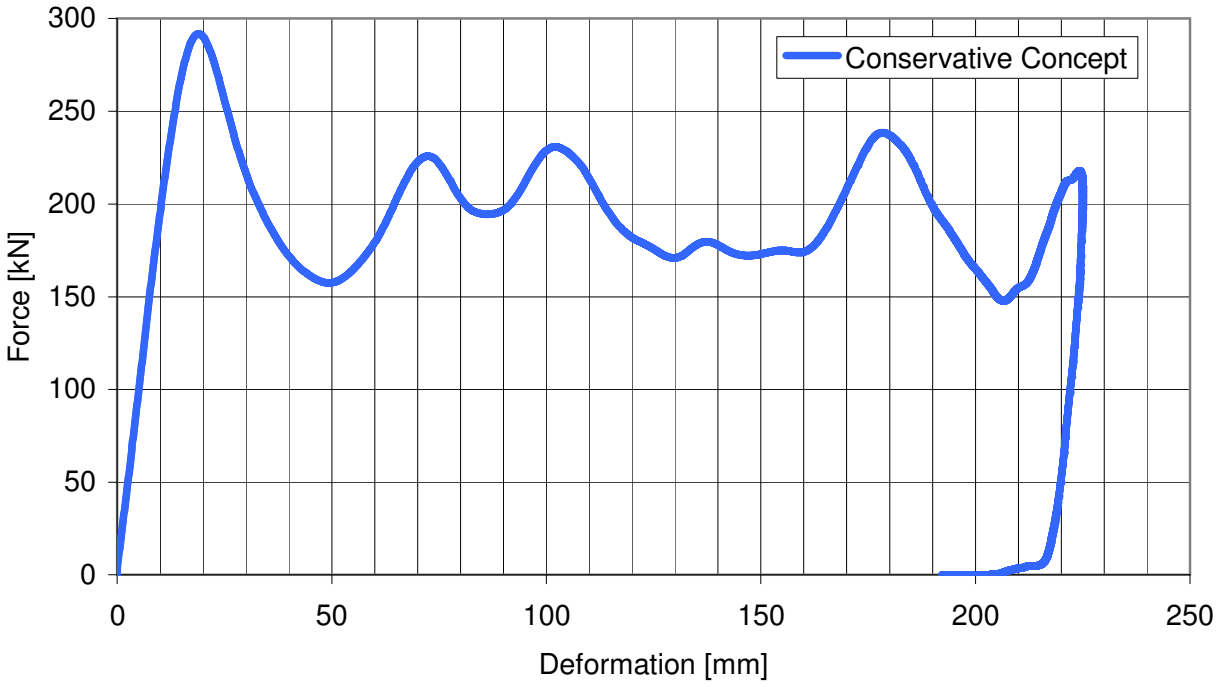

Fig. 5-6: Force versus deformation curve of conservative concept

Regarding the force-deformation-curve in Fig. 5-6, it can be observed that, like with the progressive aluminium concept, the level of energy absorption is high, since the difference between buckling load and average deformation force is relatively small.

In comparison to the progressive aluminium concept, the deformation force of the conservative concept is generally higher. This results in a higher energy absorption related to deformation. As a result, the deformation of the conservative aluminium concept that is necessary to absorb the kinetic energy is reduced to 225 mm. This means that the required deformation is 31 mm smaller than the deformation of the reference structure. This deformation reserve can be used to absorb additional energy.

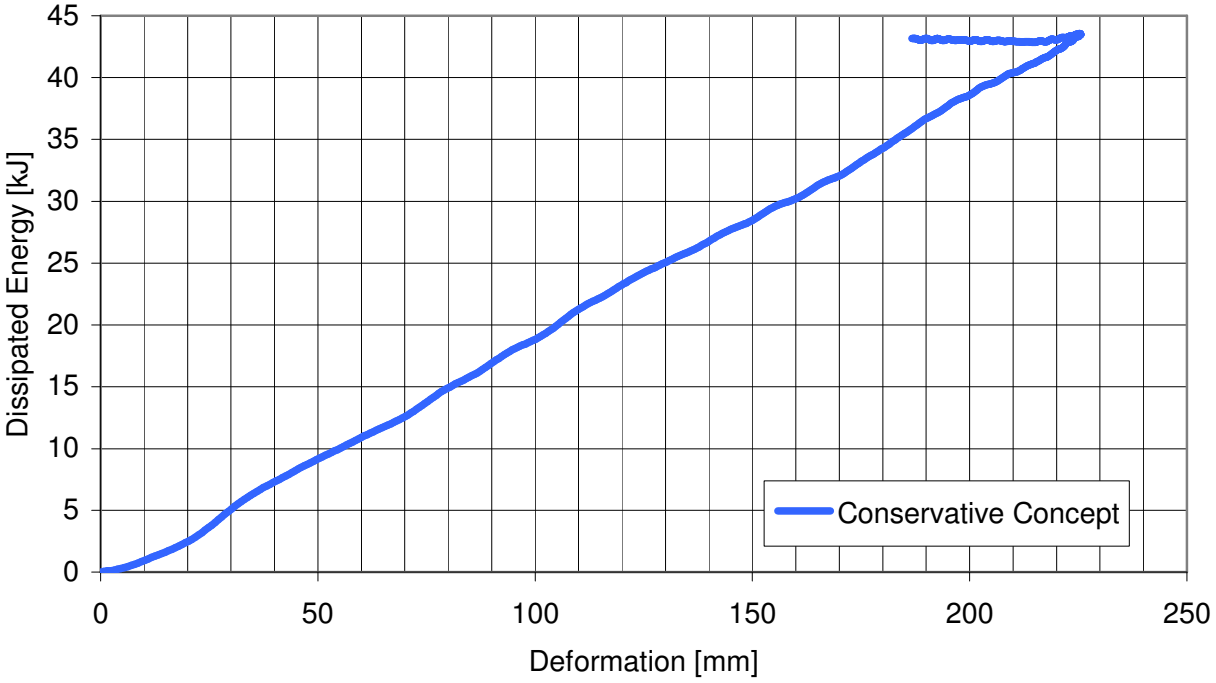

Fig. 5-7: Energy versus deformation plot of the conservative concept

Regarding the deformation behaviour, it can be observed in Fig. 5-8, that the structural integrity of the conservative aluminium front section concept is maintained throughout the entire crash. As intended, the frontal part of the longitudinal beam is deformed by regular buckling.

Buckling or even an indication for collapse is not noticed in other areas of the front section. This rigidity of the conservative concept during the crash is an additional indicator that further reduction of wall thickness, for example at the rear part of the longitudinal beam, can be considered, if decrease in performance in the critical static load case “Bending (frontal)” is tolerable.

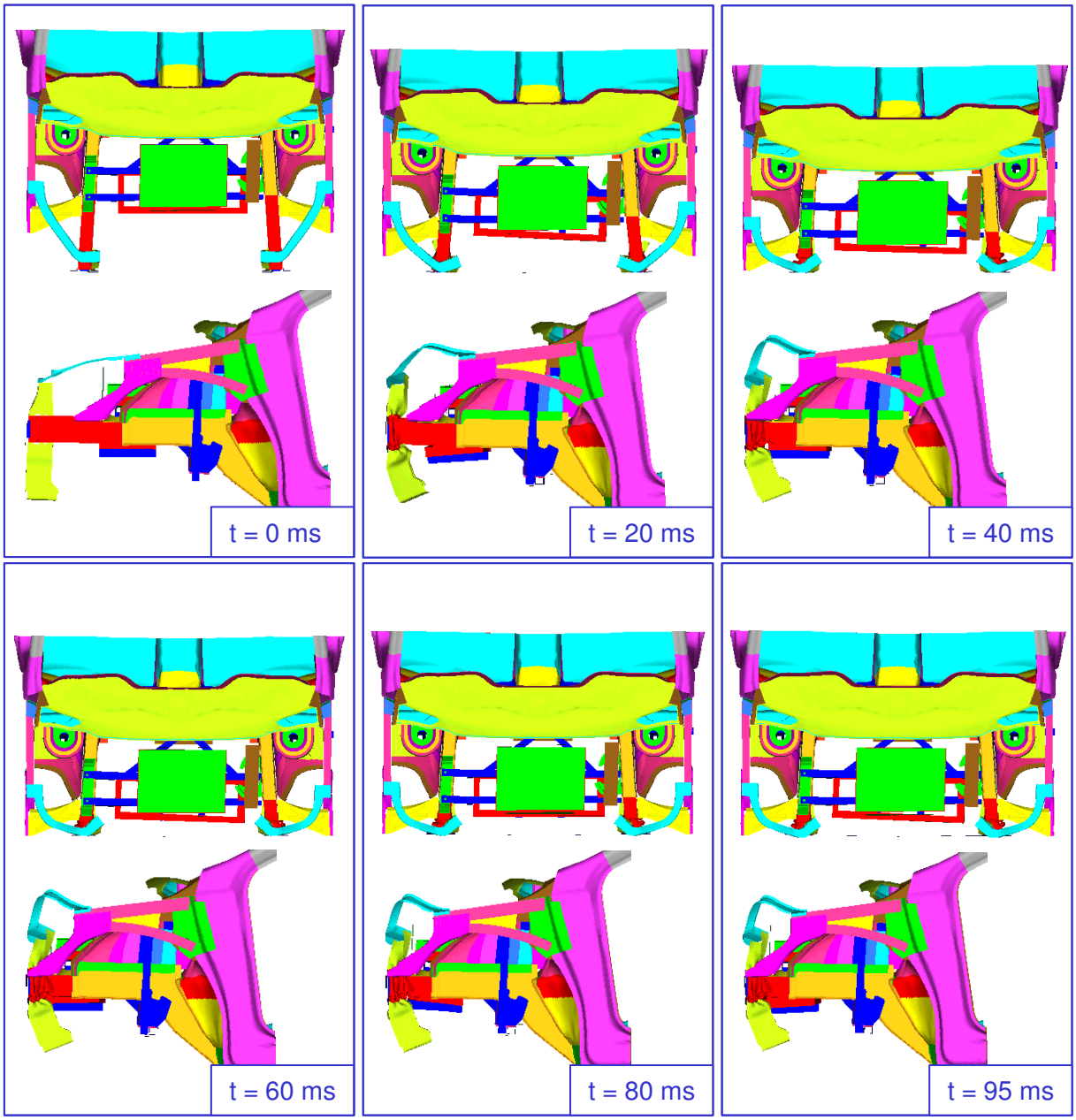

Fig. 5-8: Deformation of conservative concept (top and left view)

6 Comparison and evaluation

For the progressive as well as for the conservative aluminium front section concept the aim of this study, to achieve the same performance as the steel reference structure in the considered load cases, while reducing the weight at the best, is fulfilled. Both concepts even exceed the performance of the reference structure, although they show significant weight savings. In the following section, a final comparison of the aluminium concepts and the steel reference structure is given with respect to the weight and the performance.

For aluminium, as a lightweight material, the main focus within this study is placed on weight reduction. Fig. 6-1 shows the achieved weight reduction for the progressive and the conservative aluminium concept in comparison to the steel reference structure. The weight of the considered parts of the front section is reduced by 35 % for the conservative concept, whereas a weight reduction of 41 % is possible with the progressive concept. The higher weight reduction achieved with the progressive concept results from reduced restrictions regarding design space. The extension of the design space for the progressive concept enables the introduction of structures that are better adapted to the characteristics of aluminium and therefore allows the fulfilment of the load cases with less material usage. This underlines the common conclusion that for best possible weight saving results material substitution should always come along with appropriate changes in design.

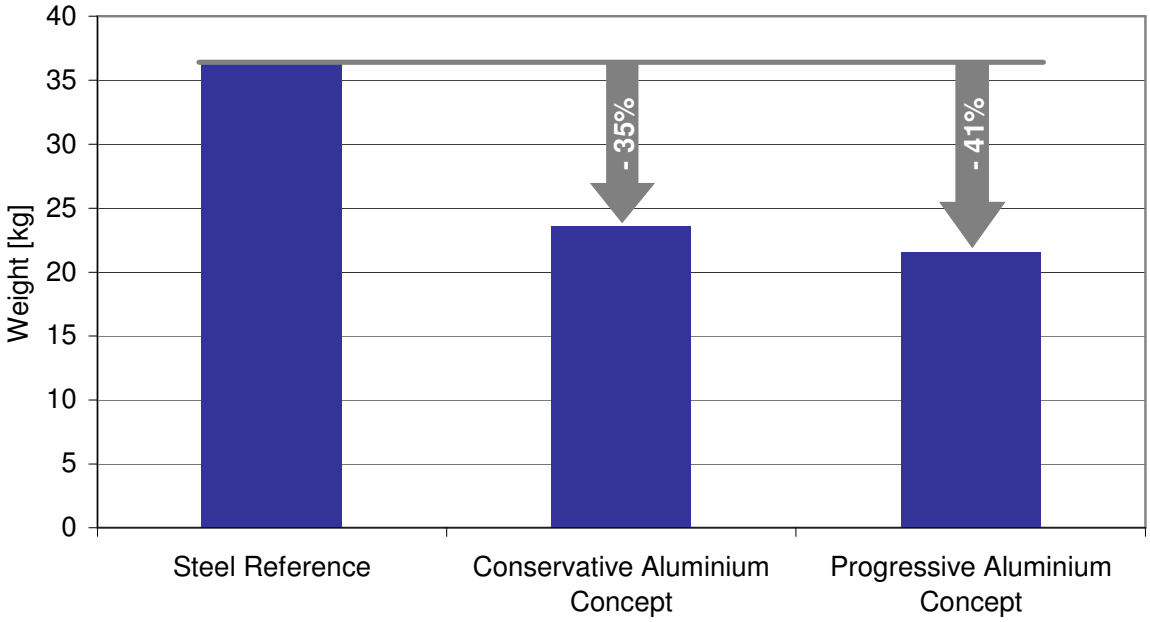

Fig. 6-1: Weight reduction achieved by use of aluminium

In addition to the reduction of weight, both aluminium concepts show an improvement in the static performance. The numerically calculated stiffness performance of the aluminium concepts and the steel reference structure is shown in Fig. 6-2. The increase in stiffness achieved by the aluminium concepts is between 7 % and 22 % depending on the load case. For the load case “Bending (frontal)” the stiffness of the reference structure is equal to both aluminium concepts. In order to guarantee the stiffness of the steel reference structure for all load cases, according to the rules of a worst case dimensioning, the aluminium concepts are dimensioned based on the load case “Bending (fontal)”. This load case is most difficult to fulfil in the aluminium concepts. In this context, it should be mentioned that this load case is of minor importance for the on-road behaviour of the complete body. If the constraints of this study, which demand at least equal performance in all load cases, do not have to be met strictly, further weight reduction, probably without noticeable decrease in performance, is possible. Besides the improvement in stiffness for three of the four considered load cases, both aluminium concepts show lower stresses in comparison to the steel reference structure for all load cases. The maximum von-Mises-stresses are reduced by 33% to 51% depending on the load case and the design concept.

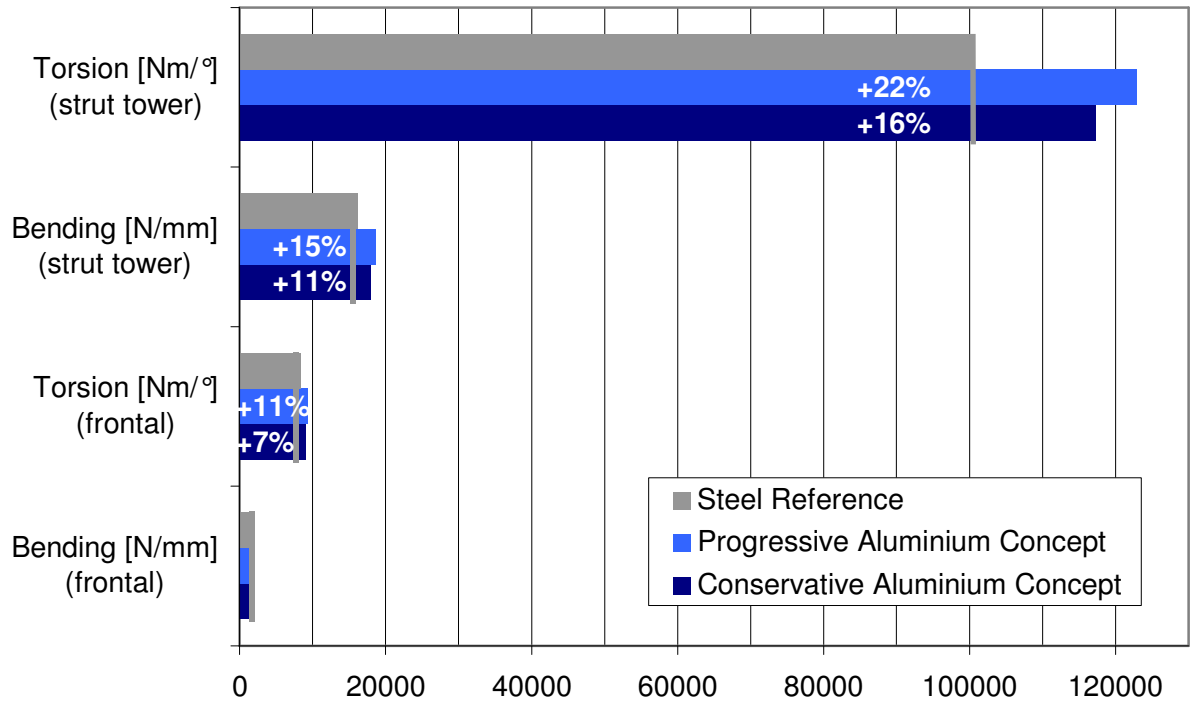

Fig. 6-2: Improvements in static performance

The comparison of the crash performances of the different front sections is not as simple as the analysis of weight reduction and static performance, since there is not a single value for the characterisation of the crash performance. All concepts are numerically crashed using the same configuration. Consequently, the energy that has to be absorbed is default and nearly the same for all concepts except for the effect of the mass savings. Qualitative analysis of the deformation plots obtained by the simulation shows that structural integrity is main-

tained throughout the entire crash for all front sections. As a result, the evaluation of the crash performance of the different front sections has to be performed based on the force-deformation-curves and the dissipated energy, shown in Fig. 6-3 and Fig. 6-4.

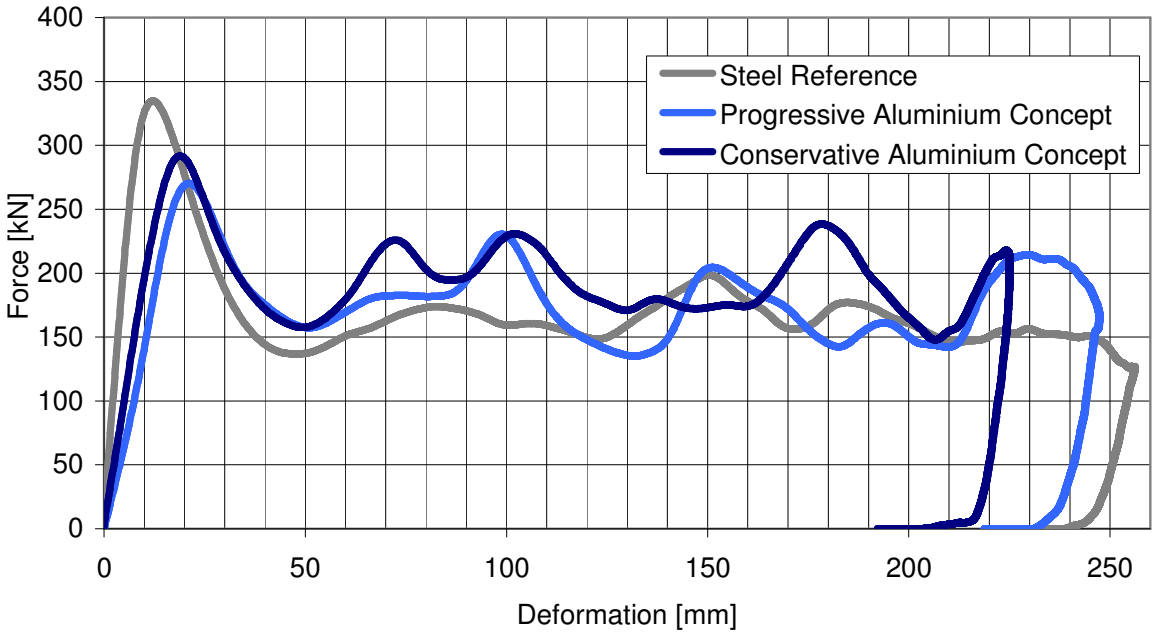

Fig. 6-3: Comparison of the force-deformation-curves

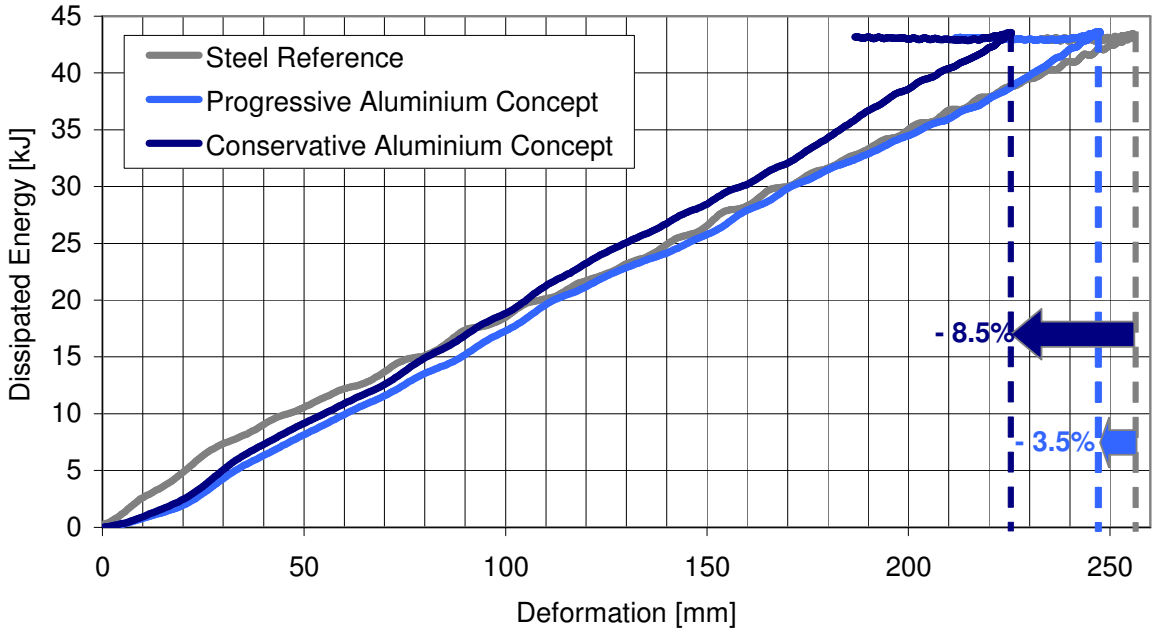

Fig. 6-4: Comparison of dissipated energies and deformation reserves

In Fig. 6-3 the curves of deformation force versus deformation for the steel reference vehicle and both aluminium concepts are compiled in one diagram. It can be observed, that in comparison to the steel reference structure, the buckling load is decreased by the aluminium concepts, while the average deformation force is increased. In theory, a small difference between buckling load and average deformation force is an indicator for good efficiency in energy absorption, since the optimum force-deformation-curve considering energy absorption efficiency is represented by a rectangle. In this respect, the conservative aluminium concept shows the best results. Nevertheless, it has to be considered, that for a complete vehicle the force-deformation-curve has to fulfil multiple requirements, including internal and external compatibility and activation of sensors. Therefore, in particular cases, high efficiency in energy absorption is not necessarily the major criterion for the adjustment of the force-deformation-curve. Since detailed information about additional requirements is not available within this study, only the efficiency of energy absorption remains as a criterion. Thus the performance of the conservative aluminium concept can be described as most beneficial among the three front sections for the considered crash load case.

Regarding Fig. 6-4, it can be observed that the energy absorbed by the front sections is at the same level, which is determined by the impact speed and crash mass. Both aluminium concepts require less deformation to absorb this energy. In comparison to the steel reference front section, the required deformation is reduced by 3.5% for the progressive and by 8.5% for the conservative aluminium concept. The remaining deformation space can be used to absorb additional energy. In this respect, the conservative aluminium concept again shows the best performance.

7 Summary

Within this study, two concepts for an aluminium front section have been developed. In comparison to a steel reference structure, a weight reduction of 35% for the conservative aluminium concept and even 41% for the progressive aluminium concept has been achieved. With an increase in static stiffness by up to 22% and an improvement in the level of efficiency in energy absorption, the structural performance of the aluminium concepts exceeds the performance of the steel structure and therefore fulfils the requirements of the study.

The concepts developed within this study are adapted to be requirements of aluminium in terms of geometry. Nevertheless, the aim of the study was not to offer guidelines for the design of aluminium front sections, but to demonstrate the mass saving potential of the material. Consequently, the level of detail in part design does not exceed a conceptual level. To enable a comparison, the parts of the steel reference model have been simplified to the same level of complexity.

In order to enable the validation of the reference finite element model, the load cases for the assessment of the structural behaviour comprise load cases that can be tested in experiments relatively easily. Deflection measurements of the longitudinal beam and a crash test with a straight impact against a planar, rigid barrier were chosen. These load cases enable only a basic comparison of the concepts and the reference structure. Nevertheless, the clearly positive results of the aluminium concepts in mass reduction and structural performance identify aluminium as a notably qualified material for structural components of the front sections of C-class passenger cars.

In contrast to the common opinion, that the crash load cases define the requirements with major influence on part thickness, the bending stiffness of the longitudinal beam has been found to be the critical load case within this study. In fact, the crash load case and the stiffness load cases with force application at the suspension-strut dome have been fulfilled using much lighter structures. Consequently, some parts of the concepts of this study are in a way over dimensioned, in order to fulfil the stiffness load case with force application at the frontal part of the longitudinal beam. This load case is of minor importance to the behaviour of the complete vehicle. For the development of a front section, not referring to the reference structure of this study, decrease in the performance of that load case should be tolerable in order to enable further weight reduction.

A multitude of interesting applications of aluminium in the front section of C-class cars has been investigated during the development process of this study. In the considered load cases and within a front section sub-system, good performance could be observed. The consideration of these ideas in a complete vehicle including a cost optimisation forms the next step. The realisation of the ideas remains a question of the manufacturer strategy, but it will also depend on the development of energy costs and the customers' preference for fuel efficient vehicles respectively.

8 Appendix

8.1 Part specification progressive concept

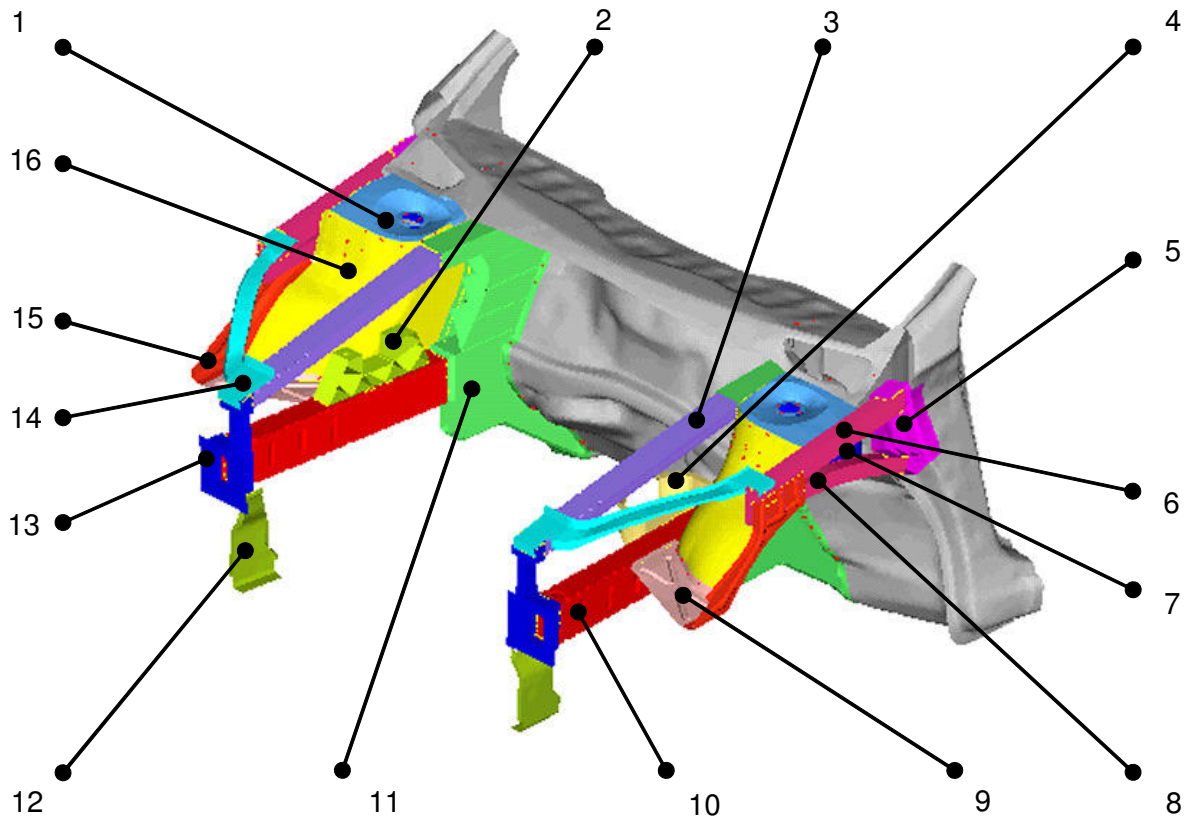

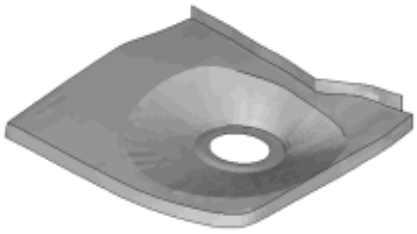

Part Specification		
Name	Strut Tower Reinforcement	
Identification	1	
Weight [kg]	0.373	
Thickness [mm]	2.55	
Material	Ac-300™ (AA 6014)	
Outer Dimensions 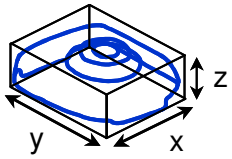	x [mm]	210
	y [mm]	245
	z [mm]	40

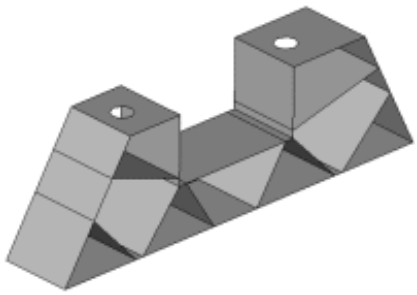

Part Specification		
Name	Engine Support	
Identification	2	
Weight [kg]	0.705	
Thickness [mm]	4	
Material	AA 6060	
Outer Dimensions 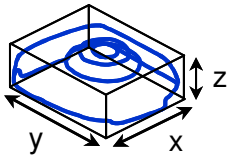	x [mm]	290
	y [mm]	55
	z [mm]	90

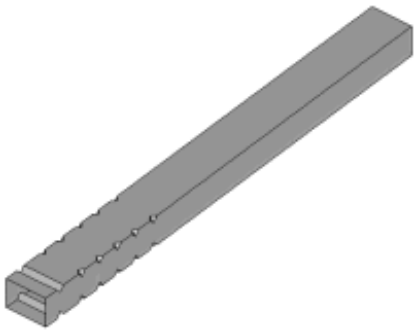

Part Specification		
Name	Upper Longitudinal Beam	
Identification	3	
Weight [kg]	0.399	
Thickness [mm]	1.2	
Material	AA 6060	
Outer Dimensions 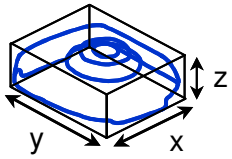	x [mm]	610
	y [mm]	65
	z [mm]	40

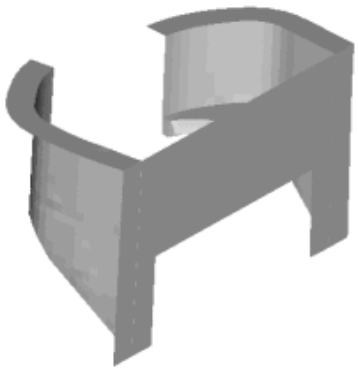

Part Specification		
Name	Gearbox Support	
Identification	4	
Weight [kg]	0.625	
Thickness [mm]	3.5	
Material	A356 (AlSi7Mg)	
Outer Dimensions 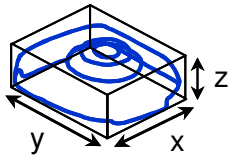	x [mm]	215
	y [mm]	50
	z [mm]	135

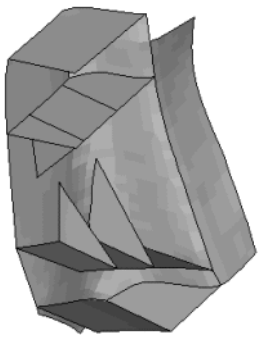

Part Specification		
Name	Outer Longitudinal Beam Support	
Identification	5	
Weight [kg]	0.522	
Thickness [mm]	3	
Material	C448™ (AlSi10Mg)	
Outer Dimensions 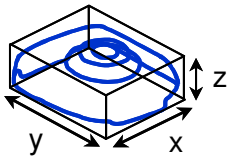	x [mm]	150
	y [mm]	50
	z [mm]	240

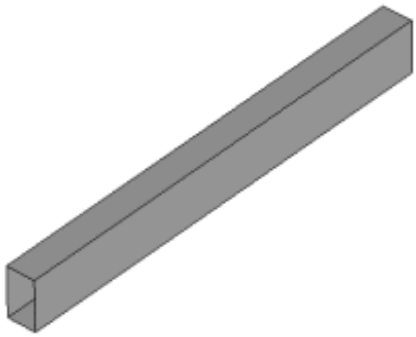

Part Specification		
Name	Outer Longitudinal Beam 1	
Identification	6	
Weight [kg]	0.327	
Thickness [mm]	1.5	
Material	AA 6060	
Outer Dimensions 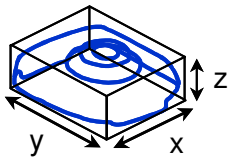	x [mm]	470
	y [mm]	35
	z [mm]	50

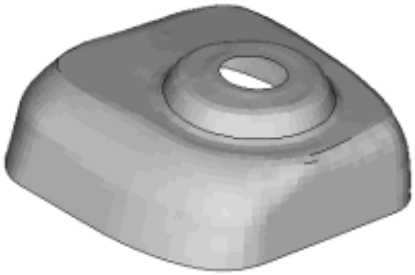

Part Specification		
Name	Strut Tower	
Identification	7	
Weight [kg]	0.78	
Thickness [mm]	3	
Material	Ac-300™ (AA 6014)	
Outer Dimensions 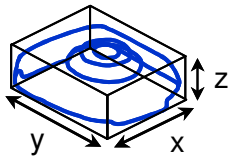	x [mm]	235
	y [mm]	245
	z [mm]	110

Part Specification		
Name	Outer Longitudinal Beam 2	
Identification	8	
Weight [kg]	0.287	
Thickness [mm]	1.5	
Material	AA 6060	
Outer Dimensions 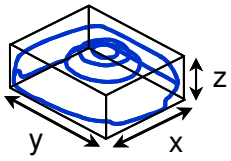	x [mm]	480
	y [mm]	35
	z [mm]	95

Part Specification		
Name	Wheel Arc Extension	
Identification	9	
Weight [kg]	0.167	
Thickness [mm]	1.58	
Material	Ac-300™ (AA 6014)	
Outer Dimensions 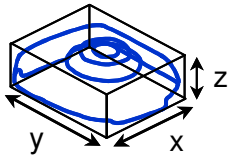	x [mm]	225
	y [mm]	260
	z [mm]	25

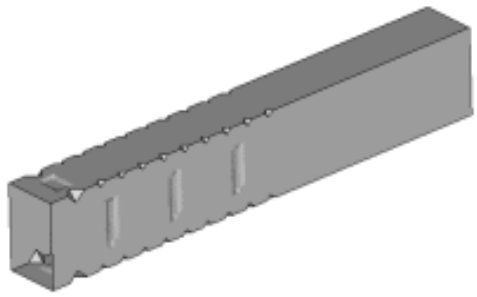

Part Specification		
Name	Longitudinal Beam	
Identification	10	
Weight [kg]	1.721	
Thickness [mm]	3.13	
Material	AA 6060	
Outer Dimensions 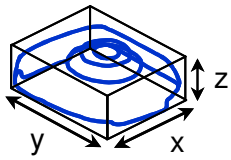	x [mm]	600
	y [mm]	65
	z [mm]	110

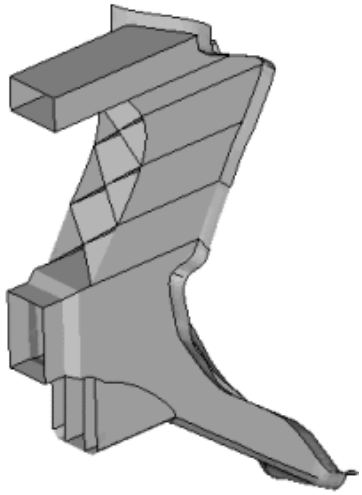

Part Specification		
Name	Main Longitudinal Beam Support	
Identification	11	
Weight [kg]	3.783	
Thickness [mm]	2 ; 5	
Material	C448™ (AlSi10Mg)	
Outer Dimensions 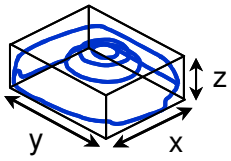	x [mm]	415
	y [mm]	115
	z [mm]	710

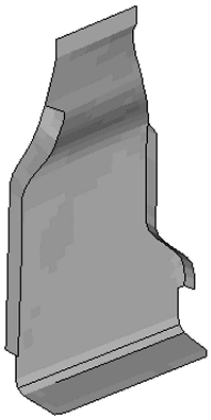

Part Specification		
Name	Frontend Support	
Identification	12	
Weight [kg]	0.125	
Thickness [mm]	1.5	
Material	Ac-300™ (AA 6014)	
Outer Dimensions 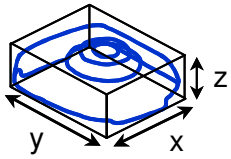	x [mm]	110
	y [mm]	35
	z [mm]	240

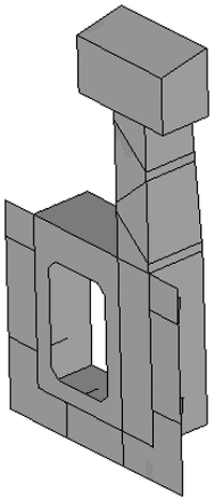

Part Specification		
Name	Front Longitudinal Beam Support	
Identification	13	
Weight [kg]	0.711	
Thickness [mm]	2 ; 5	
Material	C448™ (AlSi10Mg)	
Outer Dimensions 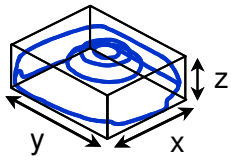	x [mm]	40
	y [mm]	145
	z [mm]	280

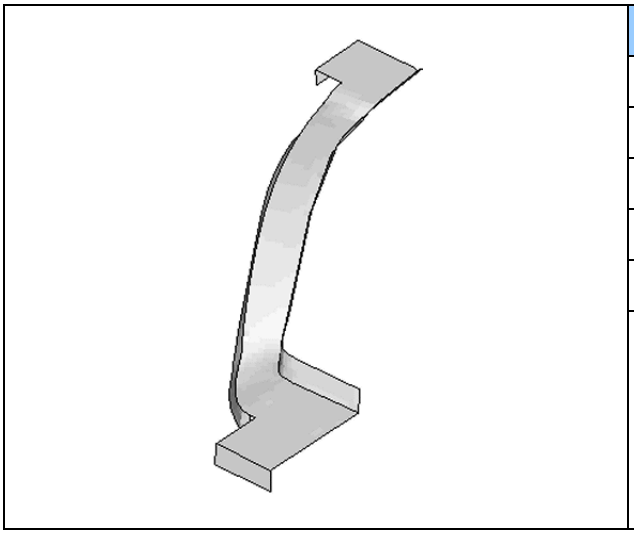

Part Specification		
Name	Headlight Support	
Identification	14	
Weight [kg]	0.115	
Material	Ac-300™ (AA 6014)	
Outer Dimensions 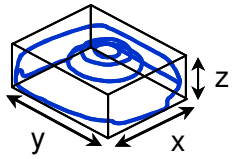	x [mm]	460
	y [mm]	340
	z [mm]	125

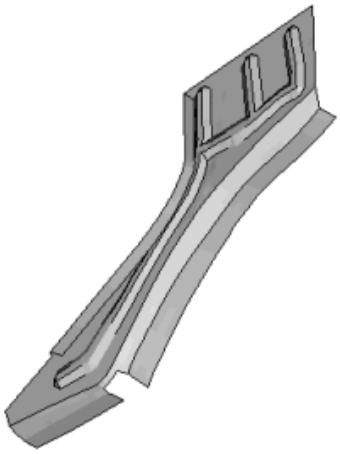

Part Specification		
Name	Outer Longitudinal Beam Extension	
Identification	15	
Weight [kg]	0.121	
Material	Ac-300™ (AA 6014)	
Outer Dimensions 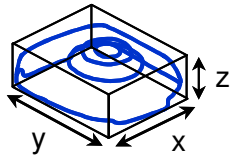	x [mm]	350
	y [mm]	30
	z [mm]	265

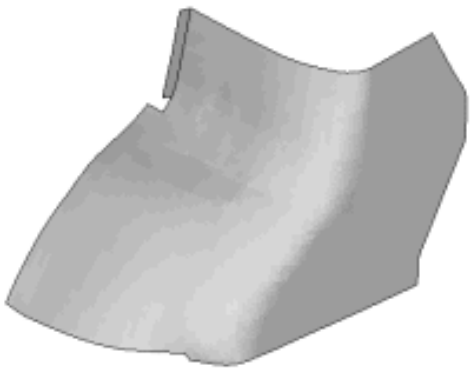

Part Specification		
Name	Wheel Arc	
Identification	16	
Weight [kg]	0.676	
Material	Ac-300™ (AA 6014)	
Outer Dimensions 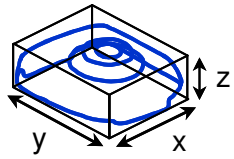	x [mm]	430
	y [mm]	280
	z [mm]	300

8.2 Part specification conservative concept

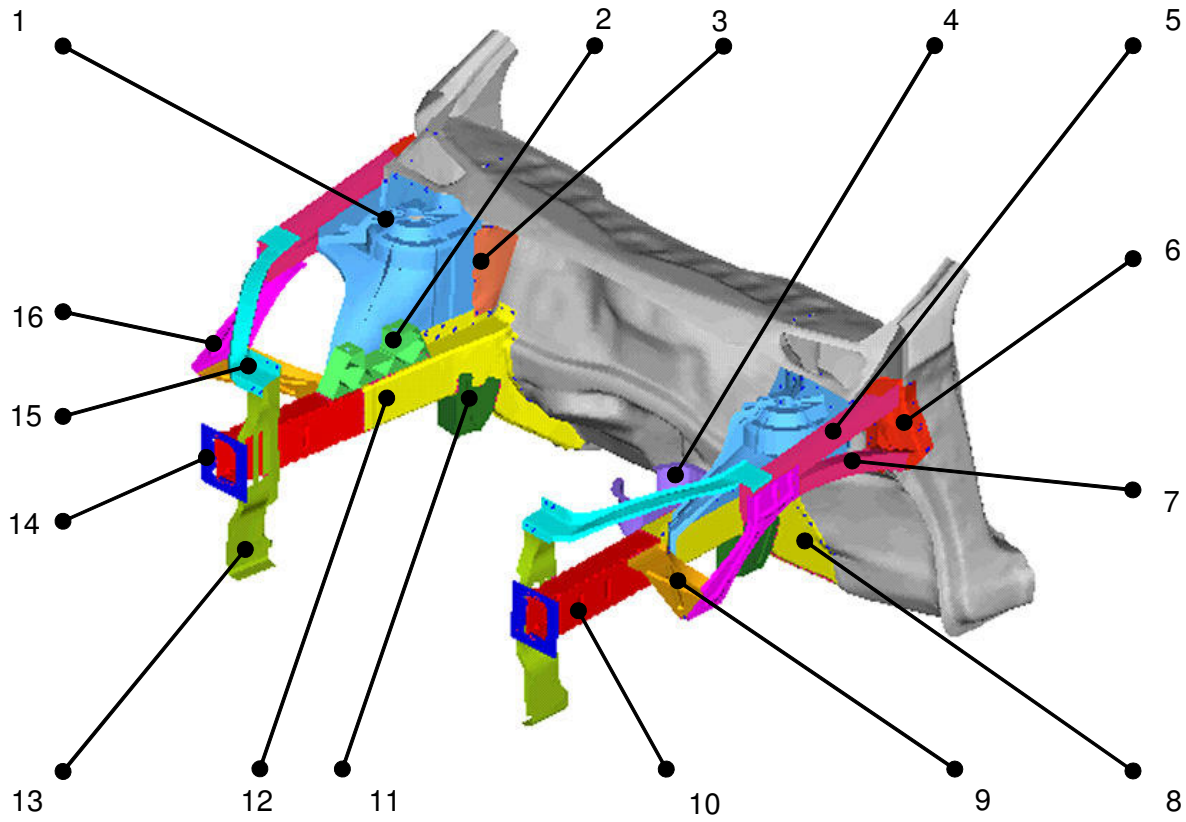

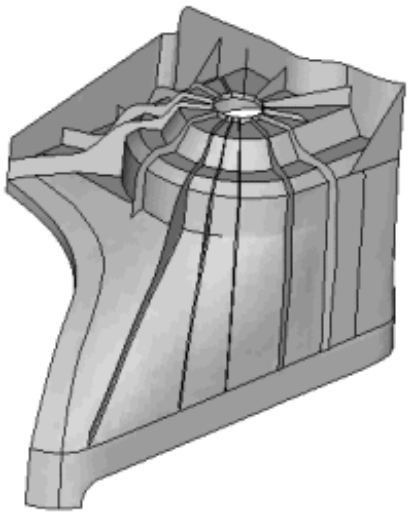

Part Specification		
Name	Strut Tower	
Identification	1	
Weight [kg]	2.292	
Thickness [mm]	2 ; 5	
Material	C448™ (AlSi10Mg)	
Outer Dimensions 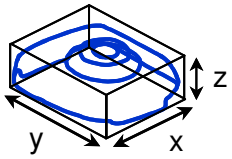	x [mm]	435
	y [mm]	260
	z [mm]	310

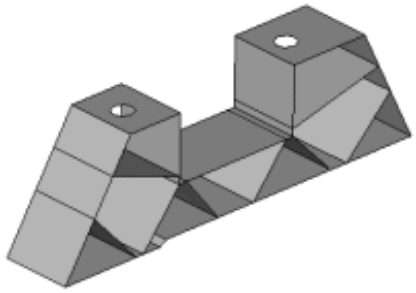

Part Specification		
Name	Engine Support	
Identification	2	
Weight [kg]	0.693	
Thickness [mm]	4	
Material	AA 6060	
Outer Dimensions 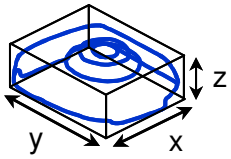	x [mm]	290
	y [mm]	55
	z [mm]	90

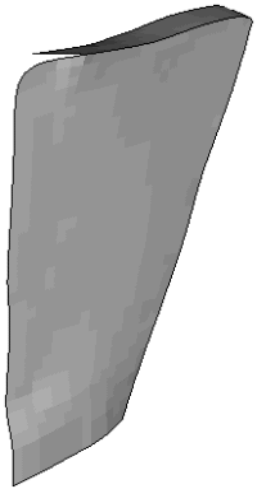

Part Specification		
Name	Strut Tower Extension	
Identification	3	
Weight [kg]	0.427	
Thickness [mm]	5	
Material	Ac-300™ (AA 6014)	
Outer Dimensions 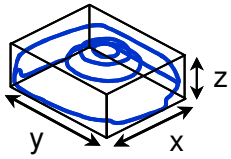	x [mm]	165
	y [mm]	30
	z [mm]	180

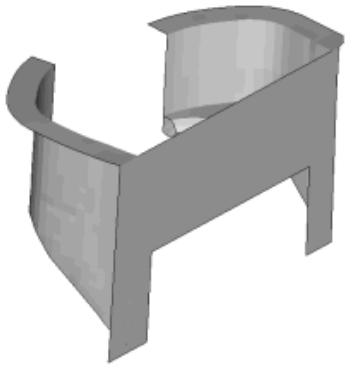

Part Specification		
Name	Gearbox Support	
Identification	4	
Weight [kg]	0.589	
Thickness [mm]	3.5	
Material	A356 (AlSi7Mg)	
Outer Dimensions 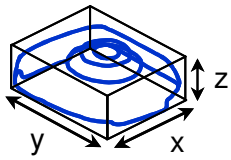	x [mm]	215
	y [mm]	50
	z [mm]	135

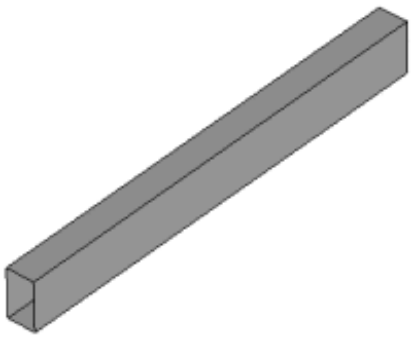

Part Specification		
Name	Outer Longitudinal Beam 1	
Identification	5	
Weight [kg]	0.373	
Thickness [mm]	1.69	
Material	AA 6060	
Outer Dimensions 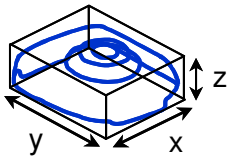	x [mm]	470
	y [mm]	35
	z [mm]	50

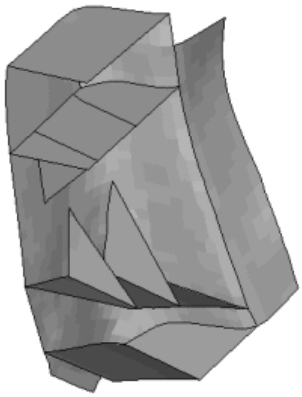

Part Specification		
Name	Upper Longitudinal Beam Support	
Identification	6	
Weight [kg]	0.562	
Thickness [mm]	3.63 ; 3	
Material	C448^{TM} (AlSi10Mg)	
Outer Dimensions 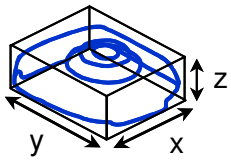	x [mm]	50
	y [mm]	150
	z [mm]	240

Part Specification		
Name	Outer Longitudinal Beam 2	
Identification	7	
Weight [kg]	0.341	
Thickness [mm]	1.69	
Material	AA 6060	
Outer Dimensions 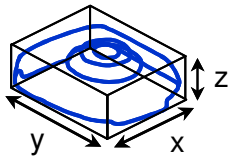	x [mm]	480
	y [mm]	35
	z [mm]	95

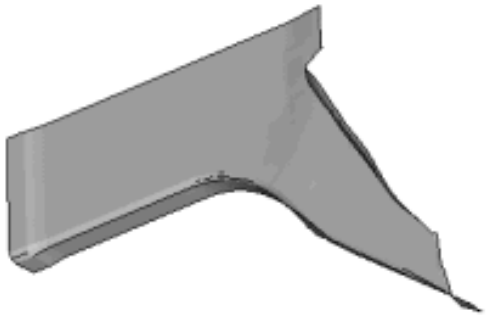

Part Specification		
Name	Longitudinal Beam 1 (Rear)	
Identification	8	
Weight [kg]	1.591	
Thickness [mm]	5	
Material	Ac-300™ (AA 6014)	
Outer Dimensions 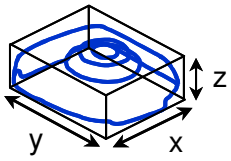	x [mm]	630
	y [mm]	90
	z [mm]	430

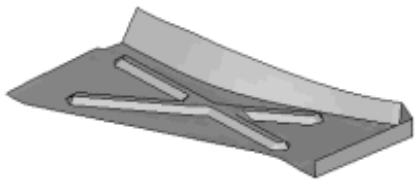

Part Specification		
Name	Wheel Arc Extension	
Identification	9	
Weight [kg]	0.474	
Thickness [mm]	5	
Material	Ac-300™ (AA 6014)	
Outer Dimensions 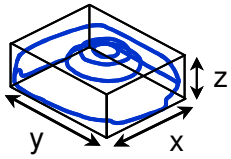	x [mm]	195
	y [mm]	265
	z [mm]	15

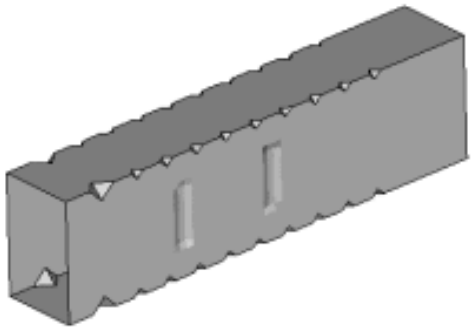

Part Specification		
Name	Longitudinal Beam (Front)	
Identification	10	
Weight [kg]	1.251	
Thickness [mm]	3.4	
Material	AA 6060	
Outer Dimensions 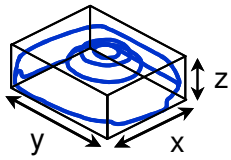	x [mm]	400
	y [mm]	65
	z [mm]	110

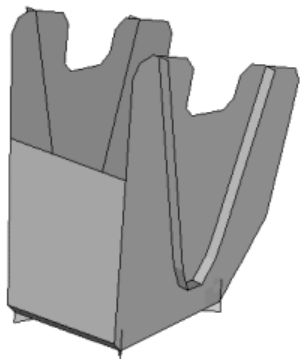

Part Specification		
Name	Subframe Support	
Identification	11	
Weight [kg]	0.505	
Thickness [mm]	3.5	
Material	C448™ (AlSi10Mg)	
Outer Dimensions 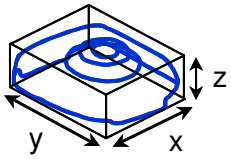	x [mm]	125
	y [mm]	65
	z [mm]	170

Part Specification		
Name	Longitudinal Beam 2 (Rear)	
Identification	12	
Weight [kg]	1.866	
Thickness [mm]	5	
Material	Ac-300™ (AA 6014)	
Outer Dimensions 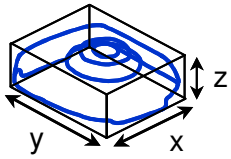	x [mm]	640
	y [mm]	115
	z [mm]	420

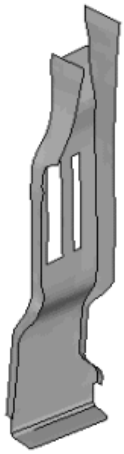

Part Specification		
Name	Frontend Support	
Identification	13	
Weight [kg]	0.385	
Thickness [mm]	2.07	
Material	Ac-300™ (AA 6014)	
Outer Dimensions 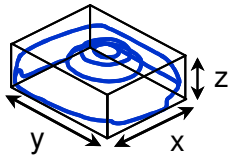	x [mm]	110
	y [mm]	50
	z [mm]	520

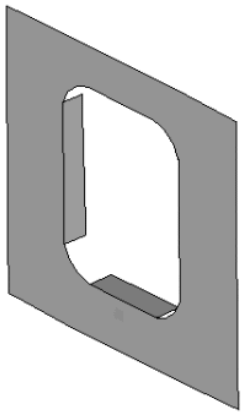

Part Specification		
Name	Crashbox Support	
Identification	14	
Weight [kg]	0.277	
Thickness [mm]	6	
Material	Ac-300™ (AA 6014)	
Outer Dimensions 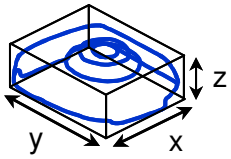	x [mm]	15
	y [mm]	145
	z [mm]	145

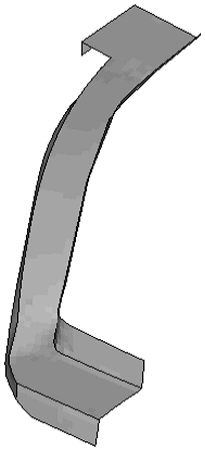

Part Specification		
Name	Headlight Support	
Identification	15	
Weight [kg]	0.566	
Thickness [mm]	5	
Material	Ac-300™ (AA 6014)	
Outer Dimensions 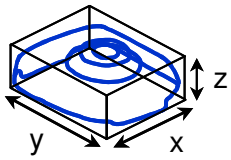	x [mm]	410
	y [mm]	340
	z [mm]	125

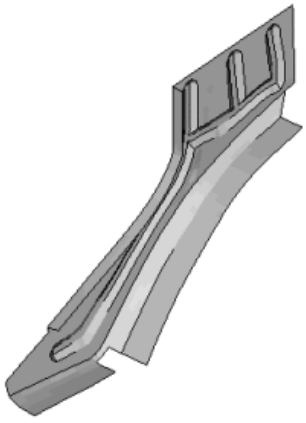

Part Specification		
Name	Outer Longitudinal Beam Extension	
Identification	16	
Weight [kg]	0.247	
Thickness [mm]	2	
Material	Ac-300™ (AA 6014)	
Outer Dimensions 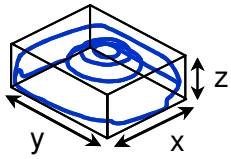	x [mm]	350
	y [mm]	30
	z [mm]	265